Available online at www.sciencedirect.com

ScienceDirect

Advances in Space Research xx (2023) xxx-xxx

ADVANCES IN SPACE RESEARCH (a COSPAR publication)

www.elsevier.com/locate/asr

Reconstructing Daily Group Sunspot Numbers Since the Maunder Minimum with Objective Inter-Calibration Algorithms

Victor Manuel Velasco Herrera[a,*], Willie Soon[b,c], Nelya Babynets[d], Judit Muraközy[b], Andrey G. Tlatov[e], Yury A. Nagovitsyn[f], Shican Qiu[g], Michal Švanda[h], Policarpo Arol Velasco Herrera[i]

[a]*Instituto de Geofísica, Radiación Solar, Laboratorio de Inteligencia Artificial, Universidad Nacional Autónoma de México, Ciudad Universitaria, 04510, Mexico*
[b]*HUN-REN Institute of Earth Physics and Space Science (EPSS), 9400, Sopron, Hungary*
[c]*Center for Environmental Research and Earth Sciences, 01970, Salem, USA*
[d]*ENP, Universidad Nacional Autónoma de México, Delegación Coyoacán, 04510, Ciudad de México, México*
[e]*Kislovodsk Mountian Astronomical Station of the Pulkovo Observatory, Kislovodsk, Kalmyk State University, Elista, 358009, Russian Federation*
[f]*Central Astronomical Observatory at Pulkovo of the Russian Academy of Sciences, Pulkovskoe Shosse 65, St. Petersburg, 196140 Russia and St Petersburg State University of Aerospace Instrumentation, Bol'shaya Morskaya ul. 67, 190000, St Petersburg, Russia*
[g]*Department of Geophysics, College of the Geology Engineering and Geomatics, Chang'an University, Xi'an, 710054, China*
[h]*Astronomical Institute of the Czech Academy of Sciences, Fricova 298, 25165, Ondrejov, Czech Republic*
[i]*Universidad Abierta y a Distancia de México, Av. Universidad 1200, Col. Xoco, Alcaldía Benito Juarez, 03330, Ciudad de México, México*

Received xx June 2013; Received in final form xx xxx 2013; Accepted xx xxx 2013;
Available online xx xxx 2013

Abstract

We present a new daily Group Sunspot Numbers (GSN) reconstruction from the Maunder minimum to Solar Cycle 24/25. This new reconstruction was obtained as a result of rectifying the raw and uncalibrated GSN database of Vaquero et al. (2016) and incorporating data from previously unconsidered GSN sources. Notably, a pivotal challenge encountered during the reconstruction of this GSN activity record, lay in the inter-calibration of different databases reported by multiple observers. The challenge is further compounded by data gaps that are particularly prevalent during the Maunder minimum. We have applied a novel methodology to solve these obstacles, entailing the calibration and standardization of all GSN databases relative to a reference observer. Our novel approach employs calibration techniques, ensuring standardized visual acuity between all individual observers. Moreover, our methodology accommodates variations in climatic, geographic, and instrumental conditions encountered by observers during their respective sunspot observations, thus establishing a uniform comparative framework. Furthermore, a comparative analysis was conducted with a total of four other different GSN reconstructions, revealing notable distinctions and resemblances that can be explained by the implementation of diverse methodologies in the respective GSN reconstruction processes and steps. In addition to the temporal differences found, both the wavelet and multi-cross wavelet analyses were carried out, which allowed a quantification of the differences and similarities in the spectral contents of various GSN records. The wavelet analysis results show the similarities and differences of the new GSN reconstruction with the inter-calibration algorithm when comparing it both temporally and spectrally with other GSN reconstructions. The periodicities of this analysis are 1.2, 5.5, 10.9, 20.6, 30.9, 58.4, and 119.8 years and 3.47, 5.4, 9.8, 27.8, 66.1, 117.8, and 160.5 days respectively.

Keywords: Keyword1 Group Sunspot Numbers ; Solar Maunder Minimum ; Solar Magnetic Activity ; Fuzzy Logic ; Wavelet Analysis ; Objective Calibration Algorithm

*Corresponding author: Tel.: +52-55-56224139; E-mail: vmv@igeofisica.unam.mx
Email addresses: vmv@igeofisica.unam.mx (Victor Manuel Velasco Herrera), soon.willie@epss.hu (Willie Soon), babynets@enp.unam.mx (Nelya Babynets), murakozy.judit@epss.hu (Judit Muraközy), tlatov@mail.ru (Andrey G. Tlatov), nag-yury@yandex.ru (Yury A. Nagovitsyn), scq@ustc.edu.cn (Shican Qiu), svanda@asu.cas.cz (Michal Švanda), arol.velasco@gmail.com (Policarpo Arol Velasco Herrera)

https://dx.doi.org/10.1016/j.jasr.xxxx.xx.xxx
0273-1177/

1. Introduction

Historical observations, instrumental data both terrestrial- and satellite-based, as well as cosmogenic isotopes have been used in reconstructing solar activity (Soon et al., 2014; Wu et al., 2018; Brehm et al., 2021; Usoskin et al., 2021; Clette et al., 2023). Sunspots forming in the solar photosphere are relatively cooler areas where the solar magnetic fields are concentrated and relatively more intense (see e.g. Solanki, 2003; Thomas and Weiss, 2004; Rempel and Schlichenmaier, 2011; Nagovitsyn, Osipova, and Nagovitsyna, 2021; Tlatov, 2022a). The use of naked-eye and telescopic sunspot observations has provided scientific information on the nature of the Sun's magnetic activity (see e.g. Spörer, 1887; Maunder, 1894; Hoyt and Schatten, 1998; Clette et al., 2014; Baranyi, and Ludmány, 2016; Švanda et al., 2016; Győri, Ludmány, and Baranyi, 2017; Hayakawa et al., 2018; Simpson, 2020; Hayakawa et al., 2021; Nagovitsyn, Osipova, and Nagovitsyna, 2021; Nagovitsyn and Osipova, 2021; Pevtsov et al., 2021; Tlatov, 2022a,b; Velasco Herrera et al., 2022a; Wang and Li, 2022; Clette et al., 2023) that, in turn, is very important for the study and understanding of space weather and Earth's climate (Hoyt and Schatten, 1997; Soon and Yaskell, 2003; Gray et al., 2010; Solanki, Krivova and Haigh, 2013; Owens et al., 2017; Pevtsov et al., 2021; Connolly et al., 2021; IPCC, 2021; Nandy et al., 2021; Connolly et al., 2023; Soon et al., 2023). Historical telescopic observations of sunspots since 1610 constitute the most direct and the longest continuous time series of Sun's activity data, while the cosmogenic isotopes from ice cores and tree rings as well as nitrate content from ice cores provide information indirectly on solar activity over centuries and thousands of years (Soon et al., 2014; Usoskin, 2017; Tlatov and Petsov, 2017; Cappellotto et al., 2022).

A particularly relevant period that has continued to confound all solar scientific communities and that has not yet had a complete and satisfactory explanation is the Maunder minimum interval of 1645 – 1715. The difficulty and complexity are mostly related to its extremely weak and anomalous solar and sunspot activity in terms of its spatial and temporal patterns (Spörer, 1887; Maunder, 1894; Eddy, 1976; Hoyt and Schatten, 1998; Soon and Yaskell, 2003; Nagovitsyn, 2007; Usoskin et al., 2015; Švanda et al., 2016; Vaquero et al., 2016). For previous analyses and the reconstruction of the annual-based group sunspot number (GSN) since the Maunder minimum see e.g., Hoyt and Schatten (1998); Vaquero et al. (2016); Velasco Herrera et al. (2022a). There are, however, still no correct nor complete reconstruction of sunspot activity during the Maunder minimum for monthly and daily resolutions.

Sunspot's drawings and historical photographs have been used to analyze the solar activity (see e.g. Galilei, 1613; Carrington, 1863; Maunder, 1894; Spörer, 1887; Ribes and Nesme-Ribes, 1993; Hoyt and Schatten, 1998; Makarov and Tlatov, 2000; Vaquero et al., 2016; Carrasco et al., 2018; Hayakawa et al., 2018, 2021; Pevtsov et al., 2021), especially to calculate the speed of solar equatorial rotation (Carrington, 1863). Historical sunspot observations are another source of information for finding different solar patterns during the Maunder Minimum (Hoyt and Schatten, 1998; Vaquero et al., 2016). But one of the difficulties in using these data for analysis is their discontinuity or gaps in recording time. In the absence of continuous sunspot observations, different interpolation methods have been used. It is important to recognize that not just any method can analyze data with gaps. Unfortunately, no interpolation has so far succeeded in a full and objective reconstruction of solar activity with a daily resolution during the Maunder minimum.

It has been often suggested that during the Maunder minimum, the solar dynamo stopped operating or functioning, and that the regular 11-yr-like sunspot activity cycle was interrupted (see for example, Charbonneau, 2020, for a detailed discussion). Furthermore, it has been speculated that certain solar phenomena, also as solar activity cycles with periodicities potentially shorter than the established 11-year cycle, may exhibit a cessation in their regular operation. These observed deviations from the expected solar activity patterns remain enigmatic, as contemporary scientific understanding has yet to provide a comprehensive physical model capable of elucidating these conjectures and puzzles. Further research and theoretical advancements are required to address

these intriguing and unexplained occurrences in dynamical variations of solar activity.

However, there are no physical reasons to suppose that the solar magnetic processes would stop or interrupted for no particular reason, and then only to be re-activated later (Velasco Herrera et al., 2022a). Conventionally the solar dynamo theory describes and attributes the solar activity cycle as a result of hydromagnetic dynamo fluid processes (Charbonneau, 2020; Brun et al., 2022).

In this study, we aim to address the unresolved issues of calibrating raw heterogeneous GSN dataset and data gaps in a comprehensive reconstruction of the history of sunspot activity as observed by multiple observers since the advent of telescopic observations. The different calibration methods proposed previously cannot be applied during the Maunder minimum due to the scarcity of solar information during this period (Clette et al., 2023).

To overcome these challenges, we employ a novel method to solve the calibration problems of the GSN databases reported by multiple observers, utilizing various instruments and operating under different meteorological and climatic conditions with observers located in very different geographical locations and observers making their observations at different times from the Maunder minimum to the present day. Accurate and objective data calibration is essential to ensuring standardization and reliability of measurements relative to a reference observer. We reported in this work one new daily and monthly reconstruction of GSN with our inter-calibration algorithms.

In this paper, we also wish to provide the important but straightforward update to the original Hoyt and Schatten (1998) database with the new 1996 to 2021 GSN data series, in daily, monthly and annual resolutions, adopted from the Pulkovo Observatory.

2. Data and Methodology

2.1. New HVP GSN composite and update to the Hoyt and Schatten (1998) GSN record

To gain a better understanding of solar activity's past and present variability, it is crucial to analyze all available solar observations. In particular, sunspot activity has continued to be reported by different observers and observatories all over the world. However, each of these observers can report varying numbers of sunspots on the same day due to differences in instrumentation, climatic conditions, and methodologies employed (see for example the database compiled by Vaquero et al., 2016). This is why there are studies that intercompare different acuities of solar observers (see e.g., Usoskin, Kovaltsov, and Chatzistergos, 2016; Karachik, Pevtsov, and Nagovitsyn, 2019). Moreover, these methodologies have not been applicable during the Maunder Minimum due to insufficient data or extended data gaps, which has made it challenging to reconstruct various GSN series.

In the World Data Center that was created for the production, preservation and dissemination of the International Sunspot Number (ISN)[1], there are also different GSN databases provided.

For the purposes of this study, we exclusively utilized all available daily time series that commenced since the Maunder Minimum. However, it should be recognized that the World Data Center does not possess an updated GSN time series that covers the full interval from 1610 to 2021. For example, the GSN series proposed by Hoyt and Schatten (1998) only spans from 1610 to 1995, while the Vaquero et al. (2016) database extends from 1610 to 2010. In addition, the daily data from this database has yet to be calibrated by those original authors probably due to the lack of applicable methodologies for handling data records with gaps.

Moreover, it is imperative to underscore that the GSN database, as presented by Vaquero et al. (2016), comprises two distinct versions (v1.12; Date: 2016-05-12 and v1.21; Date: 2020-04-19). Notably, these two versions exhibit significant disparities and inconsistencies. To commence our analysis, it is essential to address the inherent contradictions within the more recent GSN database proposed by Vaquero et al. (2016).

[1] https://www.sidc.be/silso/groupnumberv3

After analyzing both versions of the GSN database and the contributions from each observer, the results indicate that the first/original version of the GSN database (v1.12; Date: 2016-05-12) will be adopted for our HVP-GSN reconstruction. This decision is based on its larger number of observations and relatively fewer errors in the relationship between the data reported by each observer and the GSN database. In the section related to "Data Availability and Supplementary Material", a link containing the files of the two versions of database by Vaquero et al. (2016), the new GSN database, and other relevant files is provided.

Hence, the necessity arises for an updated GSN record spanning from the Maunder Minimum to Solar Cycle 24/25, i.e., 1610–2022. This new database should be subjected and open to regular and frequent updates, thereby providing the solar scientific community a convenient and free access to this invaluable dataset.

In light of such motivation, our investigation sets forth with the following objectives:

1. We have undertaken the task of creating a new composite GSN reconstruction that could be updated even on a daily basis, incorporating all the raw GSN observations that have been collected since 1610 up until the present day. As part of this effort, we have taken the initiative to correct several errors that were present in the raw original GSN database that was compiled by Vaquero et al. (2016) (and we used the v1.12 version), which in turn was a modification of the original Hoyt and Schatten (1998)'s database.
2. To update the GSN time series until 2022, we will use the active catalogue of daily GSN by the Kislovodsk mountain astronomical station of the Pulkovo observatory[2]. The Kislovodsk Solar Station of the Pulkovo observatory is located at 43° 44.77' N, 42° 31.42' E, with an altitude of 2096 m above sea level, 28 km from the city of Kislovodsk, on Mount Shat Zhad Maz.

To compose the GSN datasets spanning from 1610 to 2022, we used the daily GSN values by Vaquero et al. (2016) covering the period from 1610 to 2010, along with the GSN values sourced from the Pulkovo Observatory spanning from 1954 to 2021. We have named this revised database HVP-GSN records (i.e., after the acronym of three original datasets: Hoyt and Schatten (1998); Vaquero et al. (2016) and the Pulkovo Observatory). The added bonus of this effort will be the proper update to the original empirical GSN record of Hoyt and Schatten (1998) using the Pulkovo Observatory GSN data series from 1996 to 2021.

2.2. Algorithm for the Calibration of GSN Datasets from Non-identical Instruments and Heterogeneous Data Collected by Multiple Observers

To fully investigate and understand the nature of solar variability, continuous measurements over an extended period are required. Since 1610, sunspots have been observed discontinuously with various telescopes and by different observers. Such observational data gaps is caused by various factors with the replacement of an observer being arguably the most significant, as each observer is mortal, leading to altered quality or heterogeneous quality of observations. Additionally, all telescopes differ in aperture sizes, and it is not possible to construct and build two identical telescopes. To obtain homogenization between data obtained by different instruments, a calibration or correction coefficient can be attempted, but most of these techniques cannot be applied when there are significant data gaps such as the Maunder minimum.

In addition, there are other important instrumental factors to consider for obtaining high-quality observations of sunspots. The diameter of the objective or aperture of the telescope is critical for maximizing the amount of light collected and achieving detailed

[2] http://old.solarstation.ru/

images. Furthermore, the optical quality of the telescope is significant in terms of the precision of the shape and finish of the optical components, which ultimately affects image quality. The ratio between the focal length and the diameter of the telescope aperture is also a critical factor, as well as the stability of the telescope and temperature control to prevent thermal fluctuations in the optics of the telescope.

Weather conditions and geographical locations can also impact the quality of sunspot observations. Sky quality, measured by transparency, is among the most important weather conditions affecting observation quality. A turbulent or cloudy atmosphere, along with the amount of humidity in the air, can reduce image quality. Additionally, altitude and atmospheric turbulence can impact the quality of sunspot observations.

To achieve a consistent series of observations, various calibration methods have been proposed. One such technique involves the normalization of the data (see for example Usoskin et al., 2016). This approach has proven successful in reconstructing a series of GSN, but it is not so well applicable when there is a significant data gap, such as during the Maunder minimum.

To address this limitation, we used a standardization algorithm whereby the data is standardized with respect to a reference observer. This algorithm facilitates the calibration data from non-identical instruments and data collected by multiple observers, including instances where data gaps are present, such as during the Maunder minimum. Consult Soon et al. (2019) for more details about the algorithm.

In order to calibrate each of the individual observers (S_i) in the HVP-GSN database, which includes 738 observers represented by $i = 1, 2, 3, \cdots, 738$, with respect to the Pulkovo observatory chosen as the reference observer (r) identified as $id = 602$ according to the nomenclature of HVP-GSN database (in order to ensure consistency and prevent confusion in the future, we have chosen to retain the original nomenclature used in the Vaquero et al., 2016, database, rather than making any changes to it, while creating the new and updated HVP-GSN database) we used the algorithm proposes by Soon et al. (2019) for generating calibrated records in the presence of missing data. The algorithm is listed as follows:

$$S_i' = \frac{\sigma_r}{\sigma_i}[S_i] + [< S_r > - \frac{\sigma_r}{\sigma_i} < S_i >] \tag{1}$$

Equation (1) can be written as follows:

$$S_i' = K_i S_i + b \tag{2}$$

The calibration factor (K_i) for each observer (S_i), denoted as K_i, can be computed using the following formula: $K_i = \frac{\sigma_r}{\sigma_i}$, where σ_r represents the standard deviation of the reference observer's data ($id = 602$) and σ_i represents the standard deviation of the sunspot observations for each individual observer (S_i). Additionally, the calibration factor also involves the values of b, which is determined as $b =< S_r > -K_i < S_i >$, where $< S_r >$ represents the average value of the reference observer's data and $< S_i >$ represents the average value of each individual observer's sunspot observations. We presents the values of the calibration coefficient for each of the observers in the HVP-GSN database in the supplementary data files.

2.3. Fuzzy Logic Algorithm to Detect Outlier Data from GSN Records

In order to detect the GSN outliers found in the HVP-GSN, we have used the science of fuzzy logic (see e.g. Trillas and Eciolaza, 2015, for more details of the method) and the algorithm is implemented according to the following steps.

1. Start: Commencement of the computational sequences.
2. Data Preparation: In this stage, raw GSN data is being prepared and organized for subsequent analysis. This might involve data cleaning, normalization, and appropriate structuring and formatting.

3. Anomaly Identification: During this step, outliers or anomalies in the GSN dataset are identified. These are GSN data points that significantly deviate from the overall data pattern and could either be errors or genuinely unusual data. In some cases, the identification of atypical or abnormal data is simple and goes directly to the step of Creation of Fuzzy Rules.
4. Definition of Linguistic Variables: Linguistic variables used to describe data characteristics and anomalies are defined. These linguistic variables capture qualitative properties of the data, such as “high," “low," “normal," etc.
5. Definition of Fuzzy Sets: Fuzzy sets are created for each linguistic variable. These fuzzy sets represent different degrees of membership of GSN data to certain categories. For instance, a “high" set might have membership functions that describe how data can be “high" to varying degrees.
6. Creation of Fuzzy Rules: Fuzzy rules are formulated that establish relationships between linguistic variables. These rules define how input variables affect output variables and are based on expert knowledge or experience.
7. Fuzzy Inference: In this stage, fuzzy rules are applied to input GSN data to derive fuzzy output values. This involves combining fuzzy rules according to input contributions and obtaining results in the form of fuzzy output sets. Sometimes during this stage, the output fuzzy GSN values do not go to Defuzzification and go directly to Threshold Comparison.
8. Defuzzification: Fuzzy output sets are converted into numerical values using defuzzification methods.
9. Threshold Comparison: Thresholds are set to identify which output values will be considered outliers. Values exceeding or falling below these thresholds will be classified as outliers.
10. Filtering and Presentation: In this phase, outlier GSN data is filtered according to the set thresholds and presented appropriately for review. This may involve removal, labeling, or graphical presentation of outliers.
11. Evaluation and Adjustment: In the final step, the performance of the fuzzy logic system in detecting and handling outliers is evaluated. If necessary, adjustments to fuzzy sets, rules, or thresholds can be made to enhance the accuracy of the process.

The flowchart of the fuzzy system for detecting outliers in the HVP-GSN records is shown in Figure 1.

2.3.1. Gapped Wavelet

Information on solar activity or physical processes and mechanisms can be deduced both from temporal and frequency domains. The information of these two algebraic spaces are equivalent (Velasco Herrera et al., 2022b). We will analyze the frequency state variability of the solar photosphere with the gapped wavelet transform (W_g) because the GSN time series has data gaps in the observations ($X_g(t)$).

The classical wavelet technique (Torrence and Compo, 1998) is appropriate for analyzing times series that does not belong to linear Hilbert spaces (LHS-L_2 norm, see e.g. Velasco Herrera et al., 2022b, for a detailed discussion) as in the GSN record. But, classical wavelet spectrum can only be used for regularly spaced time series. This constraint is clearly true for the daily or monthly GSN values which often come with many observational data gaps. This is why we used the gapped wavelet (W_g) algorithm to analyze the incomplete daily GSN (see Frick et al., 1997; Frick, Grossman, and Tchamitchian, 1998; Soon, Frick and Baliunas, 1999; Soon et al., 2019, for more details on the method).

The gapped wavelet transform ($\mathbf{W}_g$) of a time series with data gaps, $X_g(t)$, is defined by Frick, Grossman, and Tchamitchian (1998) as:

$$\mathbf{W}_g(t,a) = \sqrt{\frac{1}{a\,\frac{\int_{-\infty}^{\infty} h\left(\frac{t'-t}{a}\right)\Phi\left(\frac{t'-t}{a}\right)G(t')\,dt'}{\int_{-\infty}^{\infty}\Phi\left(\frac{t'-t}{a}\right)G(t')\,dt'}}}\int_{-\infty}^{\infty}\left(\left[h\left(\frac{t'-t}{a}\right)-C(a,t)\right]\Phi\left(\frac{t'-t}{a}\right)G(t')\right)^{*}X_g(t')\,dt' \tag{3}$$

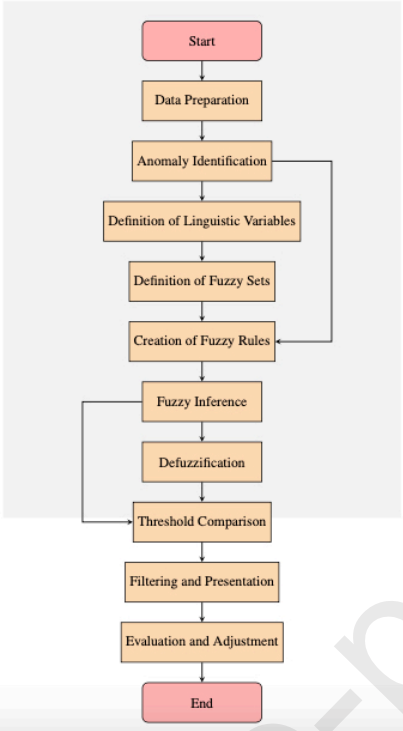

Figure 1. Fuzzy logic flowchart used to find outliers of GSN.

with

$$G(t) = \begin{cases} 1, & \text{if the signal is registered} \\ 0, & \text{lost data or not reported} \end{cases} \quad (4)$$

where t is the time index and a is the wavelet scale, the superscript (*) indicates the complex conjugate. We used the Morlet's mother function to analyse the power spectral density (PSD) of the X_g. In this case the following values $\Phi(t) = e^{(-t^2/2)}$, $h(t) = e^{iw_o t}$, and $w_o = 6$ are adopted. The global spectra show the power contribution of each periodicity inside the cone of influence (COI in the form of "U" and shown with black contours). Furthermore, the significance levels of 95% confidence in the global wavelet spectra are shown with a simple red noise model (Gilman, Fuglister, and Mitchell, 1963). The uncertainties of each periodicity are obtained according to the methodology proposed by Mendoza, Velasco, and Valdés-Galicia (2006).

The diagram of our gapped Wavelet transform algorithm is shown Figure 2, where solid arrows in either direction on the diagram represent multiplication between functions ($\uparrow, \downarrow, \longrightarrow$), the dotted arrow (::::>) represents the subtraction between functions, and $\Rightarrow$ represents the result of the gapped Wavelet transform (W_g).

2.3.2. *Temporal States of the Sun's Photosphere*

There are different methods to decompose a time series ($X(t)$) into its different oscillations. In our case, each of the oscillations represents a state of solar activity in the solar photosphere. We will use the following notation $|x(t)\rangle$, to designate each of the representation of the temporal states of the solar photosphere. The wavelet analysis shows that the spectrum is discrete and not continuous for the different solar indices from the photosphere to the solar corona. In the case of spectral analysis, $|x(f)\rangle$ represents each of the frequency states. Let us assume that for any physical system (such as the Sun), there is a finite number of discrete states and not continuous ones. Then $X(t)$ represents all temporal states of solar activity in the photosphere and can be written as follows:

$$X(t) = \sum_{i=1}^{N} |x_i(t)\rangle \quad (5)$$

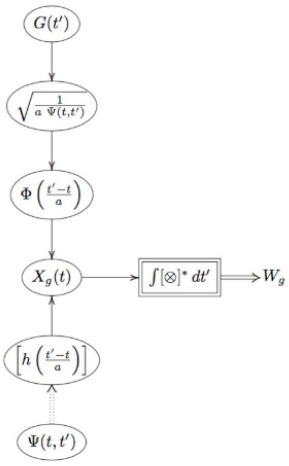

Figure 2. The schematic of our gapped wavelet transform algorithm for computing the time-frequency representative results of any underlying time series with observational data gaps.

where N is the number of states on the solar photosphere. Equation 5 does not imply that the different states of the system are orthogonal. That is, the scalar product or dot product of two different states of the system is equal to zero. In general: $\langle x_i(t)|x_j(t)\rangle \neq 0$ (where i and j represent different temporary states).

Joseph-Louis Lagrange defined the dot product of two vectors, which was later generalized to functions. Jean-Baptiste Joseph Fourier used the concept of orthogonality between functions and applied it in an integral equation (Fourier, 1822) that bears his name: the Fourier transform. It is necessary to clarify and point out that the Fourier transform should be used if and only if the time series (function or signal) belongs to the LHS-L_2. Because if this requirement is not met, the result is a spectral function, ghost function, or noisy spectrum. We suggest studying *Methods of Mathematical Physics* by Courant and Hilbert (1924, 1937) for an in-depth discussion.

In order to be able to weigh and compare different states of the solar photosphere, then we used $|\widehat{x_i}(t)\rangle$. $X(t)$ can be centralized and standardized as follows:

$$\widehat{X}(t) = \frac{1}{\sigma_x}\sum_{i=1}^{N} X_i(t) - < X(t) >= \sum_{i=1}^{N} |\widehat{x_i}(t)\rangle \tag{6}$$

where <> and σ_x are the mean value and standard deviation of $X(t)$, respectively.

In the case of the wavelet transform it is necessary that the mother Wavelet function be a complex function in order to obtain the different temporal solar states of the GSN ($|x_i(t)\rangle$). So, we use the inverse wavelet transform (Torrence and Compo, 1998) to obtain $|x_i(t)\rangle$ as:

$$|x_i(t)\rangle = \frac{\delta_j \delta t^{1/2}}{C_\delta \psi_o(0)} \sum_{j=j_1}^{j_2} \frac{\mathbf{Re}(W_n(s_j))}{s_j^{1/2}}, \tag{7}$$

where j_1 and j_2 define the periodicities range of the specified spectral bands (s_j). That is why we use the Morlet function. For the Morlet wavelet, $\delta_j = 0.6$, $C_\delta = 0.776$, and $\psi_o(0) = \pi^{-1/4}$.

Using Equations 2 and 3, we can rewrite $X(t)$ like this:

$$X(t) = \frac{\delta_j \delta t^{1/2}}{C_\delta \psi_o(0)} \sum_{n=1}^{N} \sum_{j=j_1}^{j_2} \frac{\mathbf{Re}(W_n(s_j))}{s_j^{1/2}}, \tag{8}$$

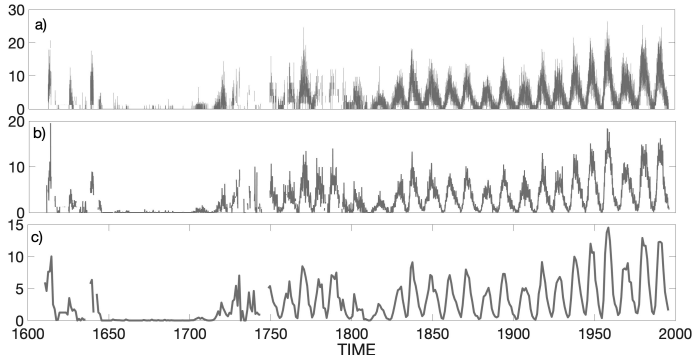

Figure 3. Time variations of the original group sunspot numbers by Hoyt and Schatten (1998) in gray line. (a) Daily, (b) monthly and (c) yearly resolutions for Solar Cycles -12 to 22 (1610–1995).

3. Results and Discussion

The initial step in our update of the GSN record involves the integration of previously missing data into Hoyt and Schatten (1998) reconstruction as proposed by Vaquero et al. (2016), complemented by the inclusion of GSN data update sourced from the Pulkovo Observatory. The significance of Hoyt and Schatten (1998) GSN reconstruction arises from its distinction as the pioneering sunspot reconstruction since the Maunder Minimum. In this preliminary update phase, the calibration factor (K) for Hoyt and Schatten (1998) GSN stands at unity ($K = 1$), denoting a one-to-one alignment with the original record. Subsequent stages of our investigation will encompass an in-depth scrutiny of alternative reconstructions. This comprehensive approach will enable a more holistic assessment of GSN variations and their implications across various reconstruction methodologies.

3.1. A Study of Previous GSN Records Including Hoyt and Schatten (1998)

Figure 3a-c shows the currently available daily, monthly and annual variabilities of the historical observations in GSN (R_g) by Hoyt and Schatten (1998) from 1610 to 1995, respectively. The three GSN records show the temporal variations of the solar magnetism in the photosphere. In addition to the lack of data, the historical reports of the GSN apparently show very complex forms and morphologies of the solar cycle in solar photospheric activity, especially in the 17th and 18th centuries. For example, the Solar Cycles -12, -11, -2, and -1 have a three-peaked shape that we have previously referred to as the Ψ shape in Velasco Herrera et al. (2022a). This peculiar shape for these solar cycles is not because of an actual interruption of the solar cycle or the solar dynamo (see Velasco Herrera et al., 2022a, for a further discussion of GSN), as has been previously hinted or suggested. The long-running study of the Sun-like stars and in particular of the Sun show that they are probably quasi-stable systems especially during the late evolutionary stage of a solar-mass sized star. This is why we venture to tentatively propose that it may not be physically possible that there are random and unknown magnetohydrodynamic fluid processes in the Sun radiative and convective zones that substantially modify the magnetic field without any explanation, such as the sudden and inexplicable interruption of the solar activity cycle during the sunspot minimum of Maunder (1645 – 1715). It is surely possible to create mathematical models and perform numerical simulations, but it does not mean that these processes exist physically in nature. Different new and recent studies have indeed shown and suggested the persistence of the solar and magnetic cycles during the Maunder Minimum (see, e.g., Makarov and Tlatov, 2000; Usoskin et al., 2015; Vaquero et al., 2015; Švanda et al., 2016; Carrasco et al., 2018).

Hoyt and Schatten (1998) reanalyzed photospheric observations to reconstruct solar activity and obtained a consistent record of sunspot activity (R_g) as a homogeneous and reliable (i.e., at least internally self-consistent) record from 1610 to 1995 (see Figure 2). Since then, R_g composition by Hoyt and Schatten (1998) has not been updated, so it is very important to update the observational

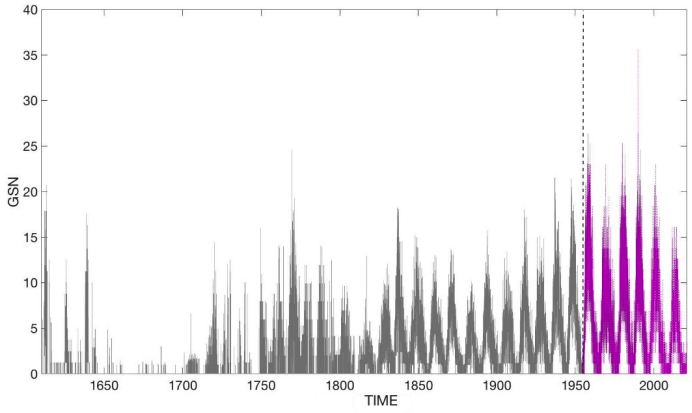

Figure 4. The daily group sunspot numbers GSN actualized. The original Hoyt database is shown with a gray line from 1610 to 1953 (i.e., Cycles -12 to 18). The Pulkovo observatory database is shown to the right of the black dotted vertical line with a purple line from 1954 to 2021 (i.e., Cycles 19 to 25).

records of the solar photosphere because it is the longest time series available for a scientific understanding of our Sun. Now, we have decided to actualize the daily GSN database (R_g) combining the original data from Hoyt and Schatten (1998) from 1610 – 1953 and then we suggested using daily data from the Kislovodsk Mountain Astronomical Station of the Pulkovo observatory from 1954 to 2022 (Nagovitsyn, Osipova, and Nagovitsyna, 2021; Tlatov, 2022b) for the purposes of cross-calibration and updates. Kislovodsk Observatory uses automatic sunspot recognition techniques (see, e.g. Tlatov et al., 2014), but sunspots with an area less than 2 μhm are not taken into account (Tlatov, 2022a). The solar observer M.N. Gnevyshev worked at this astronomical station since its foundation for 30 years.

Figure 4 shows the actualized daily R_g. From 1610 to 1953, the original Hoyt database is shown with a gray line and the Pulkovo observatory database is shown to the right of the black dotted vertical line from 1954 to 2022 with a purple line. Figure 4 also allows us to distinguish two moments of the GSN actualized. A first part is from 1610 to 1800 where gaps in the time series can be observed, particularly before, during, and after the Maunder minimum. The second part is from 1800 to 2021, which is where the GSN series can be considered complete. The calibration of the Hoyt and Schatten (1998) GSN with reference to the Pulkovo Observatory will be presented later.

If we only focus on missing GSN data rather than patterns in the solar photosphere, then our guesses may not be physically correct. For example, doubting that the solar cycle will continue during the Maunder minimum or that the solar dynamo will be interrupted. However, analyzing the GSN time series with the correct mathematical tool allows us to obtain the solar patterns even when there are data gaps in the analyzed signal. A lack of data does not mean from the point of view of signal theory that the patterns fade or disappear. Information theory and signal theory show that patterns (in this case, solar patterns) lie in different algebraically equivalent spaces, particularly in temporal and frequency spaces. Therefore, given the apparent lack of information, it is necessary to search for it or find it in other equivalent spaces. So a paradigm shift in the solar analysis consists in considering the GSN, as a relatively complete sample of the Sun's magnetic activity and not as an incomplete solar time series of the magnetized photosphere.

We particularly want to highlight that there is a substantial difference between the GSN actualized shown in Figure 4 and the international sunspot number (ISN) V2.0 of Clette et al. (2014) or even the updated version from Clette et al. (2023). While the new GSN-composite clearly shows the Modern maximum in the solar photosphere during the mid-20th century, the ISN V2.0 artificially reduced the grand Modern solar maximum by about 20%. In addition, the long-term upward trend of sunspot and solar activities

since 1700 has also been reduced in the ISN V2.0 record (see Velasco Herrera et al., 2022a, for more detailed discussion).

We also wish to add the comment that it may seem paradoxical that sunspot activity during the Maunder minimum may have been said to be "unknown" owing to the apparent lack of data. But that during the Modern maximum of the mid-20th century, with comprehensive coverage and observation both by satellite-borne instruments and by terrestrial observatories, the various versions of sunspot numbers underwent significant revisions due to the flaws in methodologies (i.e., "Locarno drift for ISN", "inflation problem for AAVSO number", etc.), and hence, the sunspot activity in this intensely monitored period is now proposed to be "unknown" or poorly determined and hence needs downward revision.

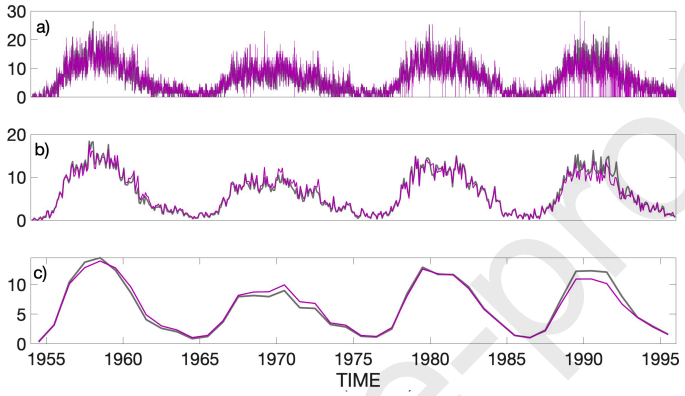

Figure 5. The comparison between the original GSN by Hoyt and Schatten (1998) in gray line and the Pulkovo observatory GSN in purple line when the two independent records overlapped from 1954 to 1995. a) daily GSN, b) monthly GSN, and c) annual GSN.

One problem may be stemming from the different consecutive series sewing together with instrumental changes (that also involved the long-term change of the human perception because human observers are part of the observing chain). Also, there is even a disagreement between magnetic field observations by different instruments on two different satellite missions: SOHO/MDI and SDO/HMI (which forced the reprocessing of MDI data by multiplying them by 1.4).

So if the historical observations of sunspots in the 17th and 18th century are questioned (Hoyt and Schatten, 1998; Usoskin et al., 2015; Zolotova and Ponyavin, 2015; Vaquero et al., 2016; Velasco Herrera et al., 2022a), then we must confront the consequences of modifying the historical sunspot data (Velasco Herrera et al., 2022a) with very little evidence. This is important because in order to understand the current solar activity variation, it is necessary to analyze the past and have probabilistic estimates of the behavior of the solar photosphere in the future. Having new and independent photospheric solar indices, such as the new GSN-composite record since 1610 in Figure 4, allows the objective analysis of the past and present of solar activity without personal biases and with the sole objective of knowing the true nature of sunspot and solar activities.

Figure 5 displays a comparison between original GSN by Hoyt and Schatten (1998), depicted in gray line, and the GSN from Pulkovo GSN observatory, represented by the purple line, during the period of overlap (i.e., 1954-1995) between the two independent records. The remarkable similarity during this period has facilitated a relatively confident update of the original Hoyt and Schatten (1998) series from 1610 to 2021. The results show that the two time series agree reasonably well especially for the monthly and annual GSN. In this comparison and internal consistency check of the two independent databases, we also have to account for the limitation[3] of the original GSN deduced by Hoyt and Schatten (1998). The correlation coefficients between these

[3]As the GSN got towards its end, there were fewer stations available to construct GSN, because in the pre-internet era, it was difficult to compile real time observations. At the end, only the NOAA Space Environment Laboratory and the British Astronomical Association observations were available. This data paucity may have caused a drift in the observations. GSN should really have about ten observers as input each year, so that criteria failed towards the end, mainly after 1992.

two GSN records shown in Figure 5 are 0.93, 0.96, and 0.98 for the daily, monthly, and annual GSN data records respectively. With the confident matching of both Hoyt and Schatten (1998) and the Pulkovo Observatory GSN records, we then simply proceed to produce the empirical update to the Hoyt and Schatten (1998) with the 1610-1995 data series remained the same but with the Pulkovo Observatory GSN records from 1996 to 2021 as the straightforward update.

3.2. Preparing For The New HVP-GSN Database

In order to derive a novel daily reconstruction of Group Sunspot Numbers (GSN) since from the Maunder Minimum to Solar Cycle 24/25, a prerequisite step involves the rectification of GSN observations in the raw data reported by Vaquero et al. (2016). Figure 6a presents the compilation of raw uncalibrated data from the original raw GSN database carried out by Vaquero et al. (2016), depicted in green line. Notably, the figure appears to indicate the technological evolution of telescopes over time, which is characterized by an increase in both the number of observers and telescopes. However, it is observed that some solar cycles, namely Cycles -3, 21, and 22, display atypical GSNs that oscillate between 30 and 58, values that are physically unrealistic.

Prior to any calibration, it is essential to correct for these anomalous values within the database. There are several approaches to address this issue, one of which is to exclude the observer (*id*) that reported these abnormal values. Here, for the purpose of identifying and confirming outlier GSN values, we have leveraged the efficacy of fuzzy logic. For a comprehensive exposition of the detailed steps, please refer to section 2.3 where a detailed elucidation of the methodology is presented. This strategic integration of fuzzy logic stands as an important new step in refining the integrity of our GSN dataset.

We discuss here one illustrative instance of outlier GSN values, serving as one representative example. For a comprehensive compilation of all rectified GSNs, please refer to the section on Data Availability and Supplementary Material. This comprehensive resource provides an extensive accounting of the corrected GSNs. For instance, the observer J.L. Rost of Nuremberg ($id = 127$) reported 35 GSN in solar Cycle -3 and made around 299 observations between 1716 and 1726.

For another example, we mention the significant issue in the two versions of the GSN databases by Vaquero et al. (2016) pertains to observer *id*=736 (i.e., T. Cragg of Los Angeles). This particular observer, who conducted observations spanning from 1947 to 2009, reported an astonishing 1,772,626 GSN observations. Such a figure is evidently not physically tenable, and it is imperative to rectify these types of errors prior to the utilization of these GSN databases. Intriguingly,Clette et al. (2023) do not document instances of such errors.

However, a direct removal this observer and their observations would result in a data sparsity problem, particularly nearing the end of the Maunder Minimum interval. Therefore, we have chosen to rehandle these abnormal GSN values using the diffuse logic algorithms (see section 2.3) that nominally locate all the maxima and eliminate them in solar Cycles -3, 21, and 22. The optimal results of the HVP-GSN are shown in Figure 6b.

The elimination of the aforementioned extreme outlying GSN values does not affect our calibration process in any way. However, it is worth noting that while some GSN values in solar Cycle -3 were eliminated, there are other GSN values that exceed those observed during the 19th and 20th centuries. Thus, it is crucial to carefully scrutinize these data before discarding them from the database. From a physical perspective, it remains unclear whether there are extremely high values of GSN after the Maunder minimum. While it is possible that this may be a manifestation of the solar dynamo's response after a prolonged period of low solar activity, it may also reflect significant issues in the collection and counting of GSN. Therefore, we have chosen to retain these "anomalous" data from solar Cycle -3 and subject them to objective analysis using our calibration methodology.

It is worth noting that while each user has the choice and ability to eliminate unrealistic values from the data, it is important to approach this task with caution and consider the potential impacts on the overall analysis. Different criteria and methodologies

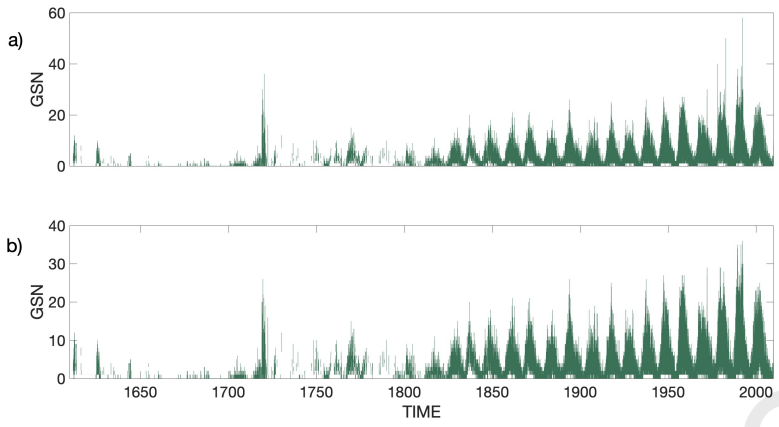

Figure 6. GSN data series. (a) The raw uncorrected GSN data collected by Vaquero et al. (2016) from 1610 to 2010 with outlier values, (b) The corrected GSN data from 1610 to 2010

for eliminating values may lead to varying results, and it is important to carefully evaluate the rationale behind each approach. Furthermore, it is advisable to document and report any such exclusions or modifications made to the data to ensure transparency and reproducibility in future analyses.

Even with a database like the one depicted in Figure 6b, it is neither mathematically nor physically appropriate to compute a daily average of the GSN values. This is because the reported GSN values are provided by different observers using different telescopes in vastly distinct geographical locations.

Moreover, we emphasize the need for a thorough correction process to make the database usable. It is somewhat surprising that Clette et al. (2023) did not address these issues, which are crucial to report to the scientific community in order to address the issue of using an incomplete and erroneous GSN database. All the corrections and clarifications that we have made can be found in the Supplementary Material.

3.3. New Reconstruction of GSNs with a Comprehensive Inter-Observer Calibration

One of the key components of the calibration algorithm (Equation 1) is the selection of the reference observer. Several criteria may be considered when selecting the reference observer. One of these criteria is to choose an observer with the most extensive solar monitoring experience and the highest number of sunspot reports, even if the observer is not currently active. For example, among the 738 observers of the HVP-GSN database, the Royal Greenwich Observatory ($id = 332$) has the highest total number of observations (i.e., 37465) and over a century of sunspot observations ($1874 - 1976$). From the perspective of the optimization theory, the Royal Greenwich Observatory is considered one of the best candidates as the reference observer. Then, all other sunspot reports from other observers can be calibrated using this reference. In fact, two of the recently published GSN reconstructions (see Usoskin et al., 2016; Chatzistergos et al., 2017, for more details) have indeed chosen the Royal Greenwich Observatory as the reference observer.

While the Royal Greenwich Observatory is an ideal selection from a solar historical perspective, our aim is to reconstruct historical sunspot observations as if all observers had the same or similar current technology. The most important criterion for selecting the best reference observer is that they are currently active and have better instrumentation than the Royal Greenwich Observatory. Furthermore, the observer reference should update their equipment regularly, which the Royal Observatory cannot do because it is not active.

This is what data calibration entails from the combined viewpoints of technological advances and both the optimization and signal processing theory. In other words, the goal is to estimate what all historical observers would have seen if they had a telescope similar to the one used by the reference observer. Therefore, we have selected the second best choice with the second longest database of sunspot reports and the second longest observation time as our reference observer of the HVP-GSN database. Consequently, all historical observations from 1610 to 2010 will be calibrated using the Kislovodsk Solar Station of the Pulkovo observatory ($id = 602$) as the reference observer. Although this observatory has reported sunspots since 1930, we will use the data from 1954 to 2022 for the purpose of our study. Calibration of all GSN data, with respect to the Pulkovo Observatory, means physically as if the reference observer was reporting the GSN "since 1610". This is the meaning of calibrating and homogenizing the 410-year long observation of GSNs based on the historical observations from all the different observers, telescopes and sky conditions. It provides a large and homogeneous database of all GSN reports ultimately allowing for a more accurate analysis and interpretation of historical sunspot observations.

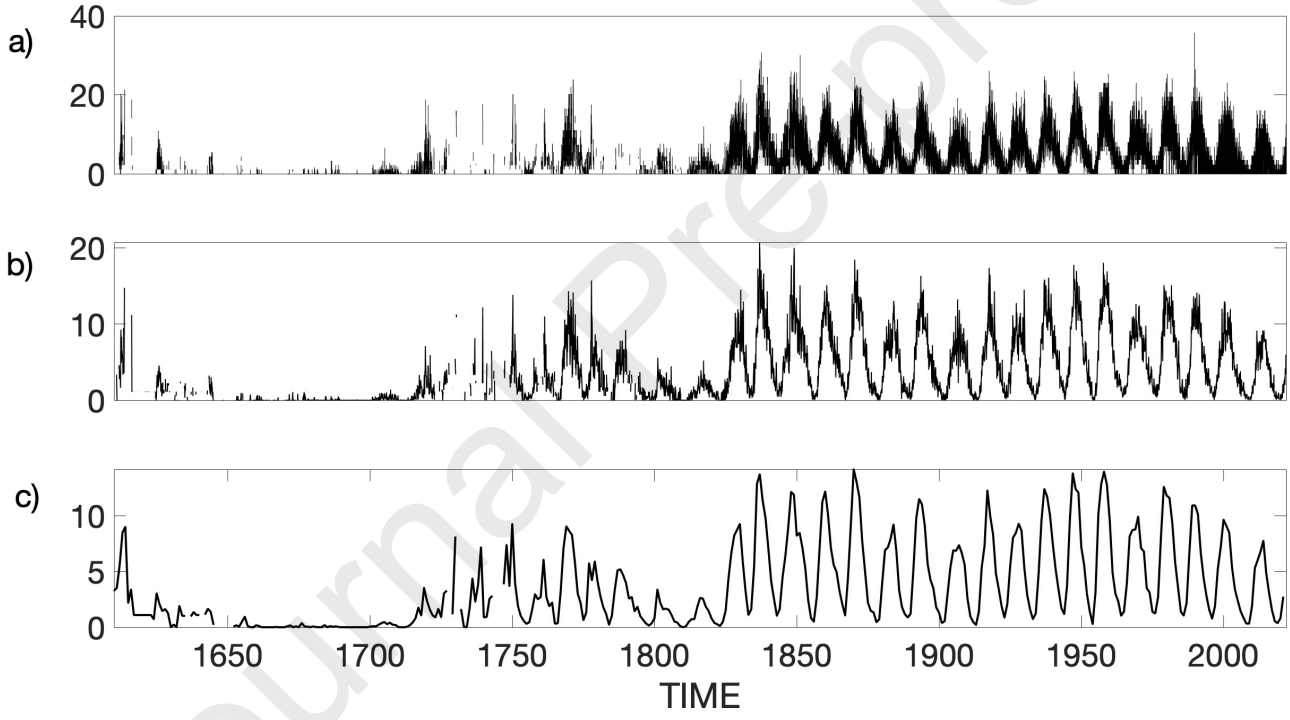

Figure 7. New reconstruction of GSN in black lines exhibit time variations that can be observed at different resolutions. Specifically, we present (a) daily, (b) monthly, and (c) yearly reconstructions for Solar Cycles -12 to 23 (1610-2008) and the beginning of Solar Cycle 24 until 2010. To generate these reconstructions, we utilized the database from Figure 6b as input data for Equation 1.

We want to emphasize that, according to the calibration algorithm (Equation 1), the data from the Royal Greenwich Observatory must be corrected by the calibration coefficient $K_{332} = 1.17$ (see the supplementary material). This means that if the Royal Greenwich Observatory had used the telescope and methodology currently employed by the Pulkovo Observatory ($id = 602$), the number of GSN observed by the Royal Greenwich Observatory would have increased by 17%. This increase represents a substantial improvement in the quality of observations, thanks to the new technologies developed for modern telescopes.

Therefore, using the Royal Greenwich Observatory as the chosen reference observer as both Usoskin et al. (2016); Chatzistergos et al. (2017) have done, would result in a 17% decrease in the current GSN data. In particular, especially during the Maunder minimum, this adjustment factor would mean a loss of solar information and a failure to fully utilize the technological advances

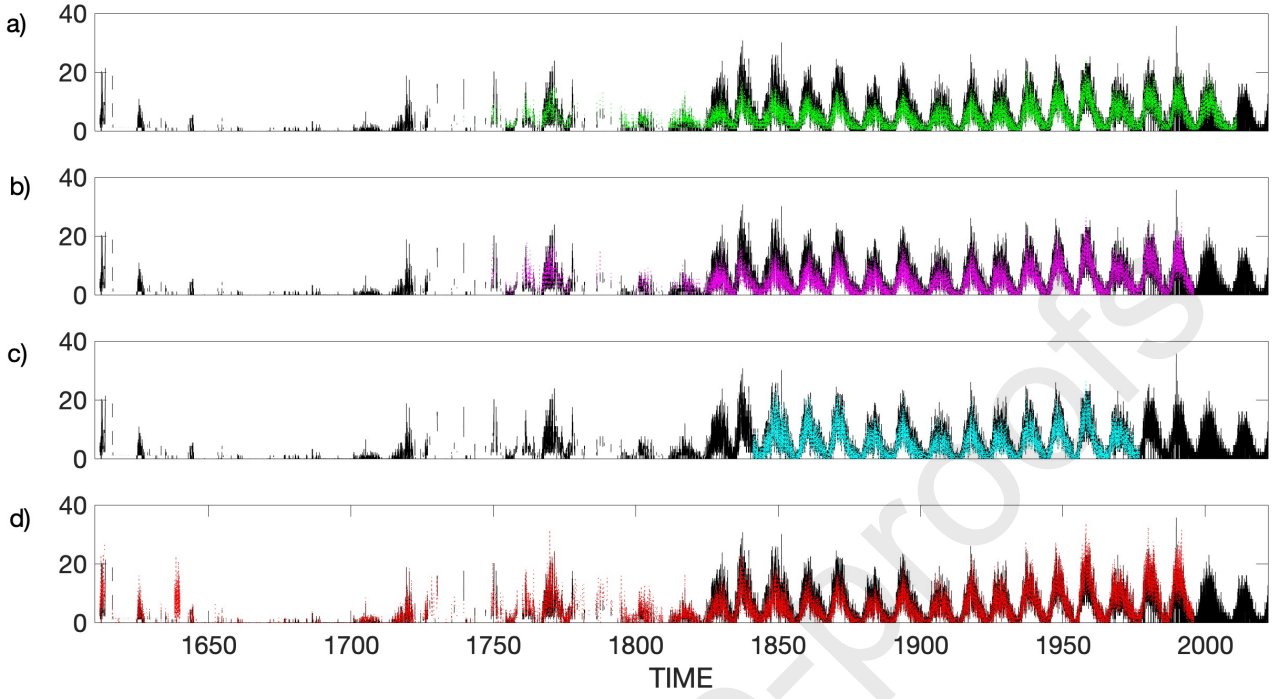

Figure 8. Comparison between our new and calibrated daily GSN reconstruction represented by a black line and: (a) GSN reconstruction of Chatzistergos et al. (2017) (green line), (b) GSN reconstruction of Usoskin et al. (2016) (pink line), (c) GSN reconstruction of Cliver and Ling (2016) (blue line), and (d) reconstruction of GSN by Hoyt and Schatten (1998) (red line).

developed over at least half a century in telescope technology. Thus, we consider that it is important to adopt the Pulkovo Observatory as the updated reference observer to calibrate all historical GSN data and obtain more observations of sunspot activity during Maunder and Dalton minima while taking full advantage of the latest advances in technology and methodology. It is important to note that not all historical observations require the same calibration coefficient, as this coefficient has been obtained according to the number of observations, mean value, standard deviation, and other fundamental characteristics of GSN observations.

The present study highlights our new GSN reconstruction achieved through the calibration of each individual historical observation comprising the complete GSN data depicted in Figure 6b, which served as input data for the inter-observer calibration algorithm. The reconstruction was performed at daily, monthly, and annual resolutions, and the results are shown in Figure 7. We wish to emphasize that the calibration process adhered to rigorous mathematical standards, strictly following the calibration approach defined by Equation 1.

Our calibration methodology provides a viable solution for obtaining a homogeneous time series, and not just probabilistic estimates of GSN, which were originally observed with telescopes of different characteristics and by different observers since the Maunder minimum (see Figure 7). To date, no other calibration methodology has been proposed for handling or even resolving this major problem (see Clette et al., 2023, for an extensive discussion on various GSN calibration issues). Importantly, our methodology does not exclude any database or observer, regardless of the uncertainties associated with their observations due to multiple factors. We have obtained an GSN database from the Maunder minimum to solar cycle 24, using a combination of analytical (inter-calibration algorithm) and statistical (diffuse logic) selection, as indeed also suggested by the most distinguished group of sunspot research experts in Clette et al. (2023). The results in Figure 7 demonstrate that our methodology enables the quantification and estimation of sunspot observation. Our algorithm has thus offered a good potential of overcoming many of the

stated limitations and difficulties rooted in the highly inhomogeneous nature of telescopic observations of sunspots and spot groups, and hence significantly enhancing our understanding of the nature of sunspots activity variations.

3.4. Reconstructing Daily Group Sunspot Numbers

To demonstrate the reliability of our inter-calibration algorithm, Figure 8 presents a comparison between our new GSN reconstruction and four different daily GSN reconstructions performed using various calibration methodologies. The comparison highlights the effectiveness of our approach in achieving an accurate reconstruction of the GSN data series. Our daily reconstruction of the GSN from 1610 to 2021 is depicted as a black line in Figure 8.

In our analysis, we first compared our newly reconstructed GSN with the previously proposed reconstruction by Chatzistergos et al. (2017), which is shown in Figure 8a as green dotted lines spanning from 1739 to 2010. While the Chatzistergos et al. (2017) reconstruction exhibits a smooth GSN series with minimal fluctuations, particularly during solar cycle peaks, this may be due to the normal distribution assumption used in their methodology. In contrast, our GSN data shows natural fluctuations, as seen in the black line. Although both reconstructions show excellent coupling between solar cycle patterns, the reconstruction by Chatzistergos et al. (2017) displays lower amplitudes for Cycles 7 to 13, possibly due to suboptimal calibration and a small number of observers. In contrast, our inter-calibration algorithm allows for the calibration of different GSN records found in the HVP databases and obtains values on the same day from different observers located in various geographical regions and climate zones. Furthermore, the methodology proposed by Chatzistergos et al. (2017) cannot be applied during the Maunder minimum. It is worth noting that our new GSN reconstruction provides a more comprehensive representation of GSN variation in both amplitude and fluctuation by utilizing all available data. Additionally, we emphasize that our calibration algorithm is not strictly a probabilistic approximation, as proposed by Chatzistergos et al. (2017) and Usoskin et al. (2016), and is discussed in further details below.

Our second comparison is with the GSN reconstruction by Usoskin et al. (2016), shown as a pink line in Figure 8b. The comparison revealed similarities and differences with our own reconstruction that are consistent with the above comparison with the Chatzistergos et al. (2017) reconstruction. The close similarities between our new reconstruction and these two previous works are expected due to the similar methodologies employed, with only minor modifications. However, our new GSN reconstruction emphasizes the use of inter-calibration and the inclusion of all available data to produce a more comprehensive and representation of GSN variation.

In our third analysis, we compared our newly reconstructed GSN with the reconstruction proposed by Cliver and Ling (2016), as shown in Figure 8c with a blue line. While there are similarities in the shape and amplitude of both reconstructions, we believe that our results offer a more comprehensive and complete understanding of the solar activity. One noticeable difference between the two reconstructions can be seen at the peak of solar Cycles 14–16, where the GSN values reported by Cliver and Ling (2016) are lower than in our GSN reconstruction.

This discrepancy could be attributed to our use of a larger number of observers and a more extensive database. Our new methodology, which incorporates inter-calibration algorithms for each GSN database found in the HVP-GSN databases, allows us to obtain the most accurate value for each observation, regardless of the observer's location or climate conditions. These improvements result in a more complete variation in both fluctuation and amplitude of the GSN, providing a more comprehensive understanding of the solar activity.

In Figure 8d, we present our fourth comparison of the recalibrated reconstruction by Hoyt and Schatten (1998), shown with red lines, covering the period from 1610 to 1995. This reconstruction is the only daily GSN reconstruction published to date, and is

analyzed during the Maunder minimum. Almost a quarter of a century after pioneering work by Hoyt and Schatten (1998), it is intriguing to compare the new information gathered for GSNs.

To our surprise, Figure 8d reveals no substantial differences between our reconstruction and the calibrated Hoyt and Schatten (1998) reconstruction during the Maunder minimum. Notably, the difference between the two reconstructions is observed for solar Cycles 7-13, where Hoyt and Schatten (1998) compiled a slightly lower number of GSNs. This difference is likely due to our reconstruction incorporating the latest information and better technology than what was available in the 1990s.

There are several additional difficulties in recording and analyzing historical sunspot data during the Maunder Minimum:

1. Lack of data: During the Maunder Minimum, solar activity decreased or weakened significantly, leading to a decrease in the number of observed sunspots. This means there are less available data to analyze during this period. Furthermore, Vaquero et al. (2016)'s recommended removal of data reported by Hoyt and Schatten (1998) from the GSN exacerbates this decrease in GSN data during this period.
2. Variations in observational instruments: Instruments and telescopes used by different observers varied in size, quality, and observation capability. This can result in inconsistent measurements of sunspots, making it difficult to compare the observed GSN values directly.
3. Lack of standardization: There was no standard protocol for observing sunspots during the Maunder Minimum. Each observer had their own method of observation and data recording, making it difficult to compare and analyze their data.
4. Data quality issues: Many sunspot records during the Maunder Minimum were made by non-professional observers and may have been affected by adverse weather conditions or lack of experience. This can result in imprecise or even incorrect measurements.

Therefore, one of the main difficulties in obtaining our new reconstruction of the GSN activity from the historical sunspot data recorded by Vaquero et al. (2016) is indeed the lack of standardization in observations and instruments used by different observers.

Standardizing historical sunspot data is a challenging task for several reasons. Firstly, historical observers used different instruments, techniques, and methodologies to measure and record sunspots, leading to significant variations in the data. Additionally, the quality of historical sunspot records may be low due to the lack of quality standards and control during the observation period.

Another difficulty is reconstructing complete time series from fragmented and dispersed historical records. Many historical records have been lost or destroyed over time, making it difficult to establish an accurate chronology of sunspots. Additionally, some records are incomplete or have gaps due to the lack of observations or interruptions caused by external factors such as wars, natural disasters, or other unforeseen and even technical problems.

Standardizing historical sunspot data may also require error correction or removal of outliers, which can be difficult to do without detailed information about observation conditions and methodology used in each case. Standardization refers to the process of adjusting data to make them comparable. In the context of historical sunspot data, this involves adjusting measurements to be consistent over time and between different observers and telescopes.

Some common standardization techniques include normalization, trend correction, outlier removal, interpolation, and extrapolation. These methods can help adjust data to more accurately reflect real variations in solar activity over time, enabling more precise comparison between different datasets and the detection of long-term trends. However, these methods cannot be applied to the Maunder Minimum.

Nonetheless, we have now proposed a standardization of historical sunspot data (Equation 1) using a single chosen reference observer, and the results show that it can be a solution to this great challenge due to the heterogeneity in observation and measurement

methods used by different observers over time. Our monthly GSN reconstruction can now be compared with other GSN products and independent reconstructions.

3.5. Reconstructing Monthly Group Sunspot Numbers

We present the comparison with the monthly reconstruction from Chatzistergos et al. (2017), which is illustrated with green lines in Figure 9a spanning from 1739 to 2010. We observe a notable concordance in morphology between both reconstructions, spanning from solar Cycle 14 through Cycle 23. It is however apparent that reconstructed GSN values by Chatzistergos et al. (2017) are lower from solar Cycle 8 to Cycle 13. This relatively lower GSN values in Chatzistergos et al. (2017) record is potentially caused by the exclusion of several observers, particularly the early observations of the Royal Greenwich Observatory.

In contrast, our methodology includes all available observers, including those of the Royal Greenwich Observatory. While some may wish to assume the poor quality of observations from this well-known Observatory at the onset of their sunspot observation operations, we posit that such an assumption equates to a dismissal of all pre-1900 observers, including Wolf and classify them as erroneous observers.

Therefore, we wish to highlight the integrity of our reconstruction, given the incorporation of all data and the determination of correction coefficients for each observer. From an information perspective, multiple primary observers equate to a lack of quality in all observers, thereby augmenting dispersion and uncertainty. In addition, it can be appreciated that another difference in the methodology proposed by Chatzistergos et al. (2017) is that, during the solar Cycle minima 0 to 6, their reconstruction remains constant and does not reach the minima values reported by most observers in Vaquero et al. (2016). Moreover, it is incorrect to assume a normal distribution of sunspots, as postulated by the methodology of Chatzistergos et al. (2017), due to the asymmetry of the onset and end of each solar cycle. It should also be noted that this methodology cannot be applied in periods with scarce or very scarce GSN data, such as the Maunder Minimum. In contrast, our method of reconstruction of GSN can be applied at any time, including the Maunder minimum, which constitutes one of its distinctive advantages.

In order to continue evaluating our new GSN reconstruction, we performed a second comparison with the reconstruction by Usoskin et al. (2016), which is represented by a pink line in Figure 9b. The similarities and differences with our own GSN reconstruction are very similar to those described previously with the reconstruction by Chatzistergos et al. (2017). This is because both reconstructions utilized a very similar methodology, albeit with some minor changes. However, it is important to highlight a substantial difference between our GSN reconstruction and the reconstruction from Usoskin et al. (2016), which is not observed in the reconstruction from Chatzistergos et al. (2017). This difference pertains to the high GSN values in solar Cycles 19, 21, and 22, compared to our GSN reconstruction. This discrepancy could be attributed to the correction coefficient utilized by Usoskin et al. (2016).

We conducted a third comparison with the GSN reconstruction from Cliver and Ling (2016), which is shown in Figure 9c with a blue line. The similarities in the shape and amplitude of both reconstructions are not coincidental, as Cliver and Ling (2016) utilized the database from the Royal Greenwich Observatory. However, a slight difference between the two reconstructions is observed at the peak of the solar Cycle 16, where the GSN values reported by Cliver and Ling (2016) are lower when compared to our GSN reconstruction. This could be attributed to our utilization of a larger number of observers, thereby rendering our reconstruction more comprehensive and complete in this regard.

Finally, the fourth comparison we make in Figure 9d is with the already-calibrated reconstruction by Hoyt and Schatten (1998), which is illustrated with red lines spanning from 1610 to 1995, utilizing Equation 1. Although Vaquero et al. (2016) reported that different observations included in the original database of Hoyt and Schatten (1998) were eliminated, Figure 9d does not show

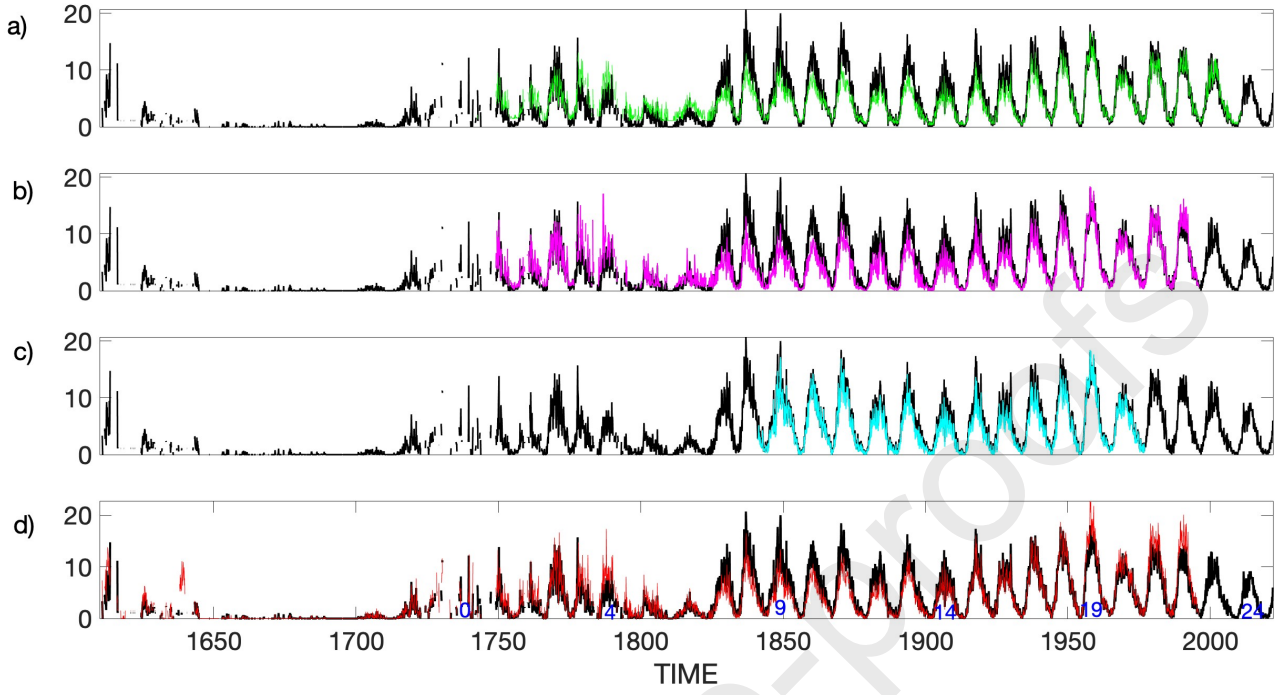

Figure 9. Comparison between our new and calibrated monthly GSN reconstruction represented by a black line and: (a) GSN reconstruction of Chatzistergos et al. (2017) (green line), (b) GSN reconstruction of Usoskin et al. (2016) (pink line), (c) GSN reconstruction of Cliver and Ling (2016) (blue line), and (d) reconstruction of GSN by Hoyt and Schatten (1998) (red line).

there is any substantial difference between these two reconstructions. The main difference in methodology is that we used only one reference observer, while Hoyt and Schatten (1998)'s reconstruction was calibrated using multiple observers. However, the results show that the calibrated reconstruction of Hoyt and Schatten (1998) is very similar to ours. The close similarity between our reconstruction and the calibrated reconstruction from Hoyt and Schatten (1998) is likely due to the fact that both utilize different observatories as the basis for their reconstructions, with a correction coefficient of 1.17 between the Royal Greenwich Observatory used by Hoyt and Schatten (1998) and the Pulkovo Observatory used in our study.

One additional difference between the two reconstructions is that Hoyt and Schatten (1998) reported higher GSN observations in solar Cycles 19, 21, and 22, which interestingly also agrees with the results of Usoskin et al. (2016), who utilized a very different methodology from that of Hoyt and Schatten (1998).

In summary, our comparison of different reconstructions reveals that the choice of reference observer is a crucial factor in the reconstruction of GSN activity time series. Furthermore, a larger number of primary observers is likely to increase the divergence between different reconstructions.

Figure 10 depicts a comparison between our annual GSN reconstruction, represented by a black line, and the three other reconstructions compared for the daily and monthly resolutions in Figure 8 and 9, respectively.

3.6. Reconstructing Annual Group Sunspot Numbers

In Figure 10a, we present a comparison between our annual GSN reconstruction and that of Chatzistergos et al. (2017), represented by a green line. An excellent synchronization between both reconstructions is observed from solar Cycles 19 to 23, while a lower GSN values from solar Cycles 7 to 18 is reported by Chatzistergos et al. (2017). Importantly, there is a significant concordance in the solar minima between both reconstructions from solar Cycles 7 to 23. However, for solar Cycles 0 to 6, the reconstruction by

Chatzistergos et al. (2017) did not reach the bottom of each solar minimum, with relatively higher GSN values during solar maxima in these same cycles. This notable discrepancy is possibly attributable to the calibration coefficients used and the limited use of GSN data applied in Chatzistergos et al. (2017)'s methodology, in contrast to the employment of all available information in the HVP-GSN database and an objective algorithm used in our new reconstruction.

In Figure 10b, the second comparison of our reconstruction with Usoskin et al. (2016)'s reconstruction is presented with a pink line. Overall, the annual behavior is very similar to the previous analysis of annual GSN produced in Chatzistergos et al. (2017), which is expected given the similarity in methodology between these two reconstructions by similar authors.

It is worth noting that reconstructions by Chatzistergos et al. (2017) and Usoskin et al. (2016) have been extensively used in the scientific community, and its comparison with our reconstruction allows for a better assessment of the quality of our results. This comparison also reveals that our reconstruction is consistent with one of the most widely used GSN reconstructions in the field, further validating our approach. A notable difference in our reconstruction compared to the other analyzed reconstructions is the high fluctuations observed in the descending phase of solar Cycles 3 to 5, which are not present in any of the other reconstructions.

In the third comparison (Figure 10c), the Cliver and Ling (2016)'s reconstruction is presented with a blue line. Overall, an excellent synchronization can be observed between both reconstructions. The small differences are shown in solar Cycles 13 to 18, where Cliver and Ling (2016) reports a relative lower GSN values.

The last comparison is shown in Figure 10d. In this fourth comparison, it is made with the Hoyt and Schatten (1998)'s reconstruction, which is shown with a red line. The first difference observed in the Hoyt and Schatten (1998) reconstruction is the shape of solar Cycles 3 and 4, which is very different from all other reconstructions analyzed here. A great coincidence is, however, notable for solar Cycles 5 and 6. Furthermore, Hoyt and Schatten (1998) reported lower GSN values for solar Cycles 7 to 13. While from solar Cycle 14 to 18, as well as solar cycle 20, there is great synchronization. Finally, for solar Cycles 19, 21, and 22, a higher number of GSN are reported by Hoyt and Schatten (1998). These differences between these two reconstructions are due to the data revisiting in the Vaquero et al. (2016) database, as well as the different calibration coefficients and methodologies used in these two GSN reconstructions.

It is important to note that each reconstruction has its strengths and limitations and understanding these factors and issues is crucial for the interpretation of results. In this study, we compared our reconstruction with four other primary GSN reconstructions to provide a comprehensive assessment of both the agreements and discrepancies among them, which can help to better understand the evolution of solar activity over the past four centuries.

It is interesting to observe how different solar reconstructions can vary slightly in some details, such as the amount of reported sunspots in certain cycles. These small differences may be the result of variations in the methodology used by each study, as well as in the quality and quantity of the data used for the reconstruction.

However, despite these variations, it is encouraging to see that in general, all reconstructions agree on the most important patterns of solar activity and the most significant changes in solar activity over time. These comparisons are a valuable tool for improving our understanding of the behavior of the Sun and for validating models and theories about the solar cycle and its impact on our climate and technology. Our new GSN reconstruction presented in this study was developed using an innovative methodology that allowed for standardization of all GSN data reported by different observers, resulting in greater accuracy in calibration. In addition, data from new sources that had not been considered in previous reconstructions were incorporated. These improvements allowed us to obtain a GSN reconstruction with higher temporal resolution and greater reliability in the GSN values reported.

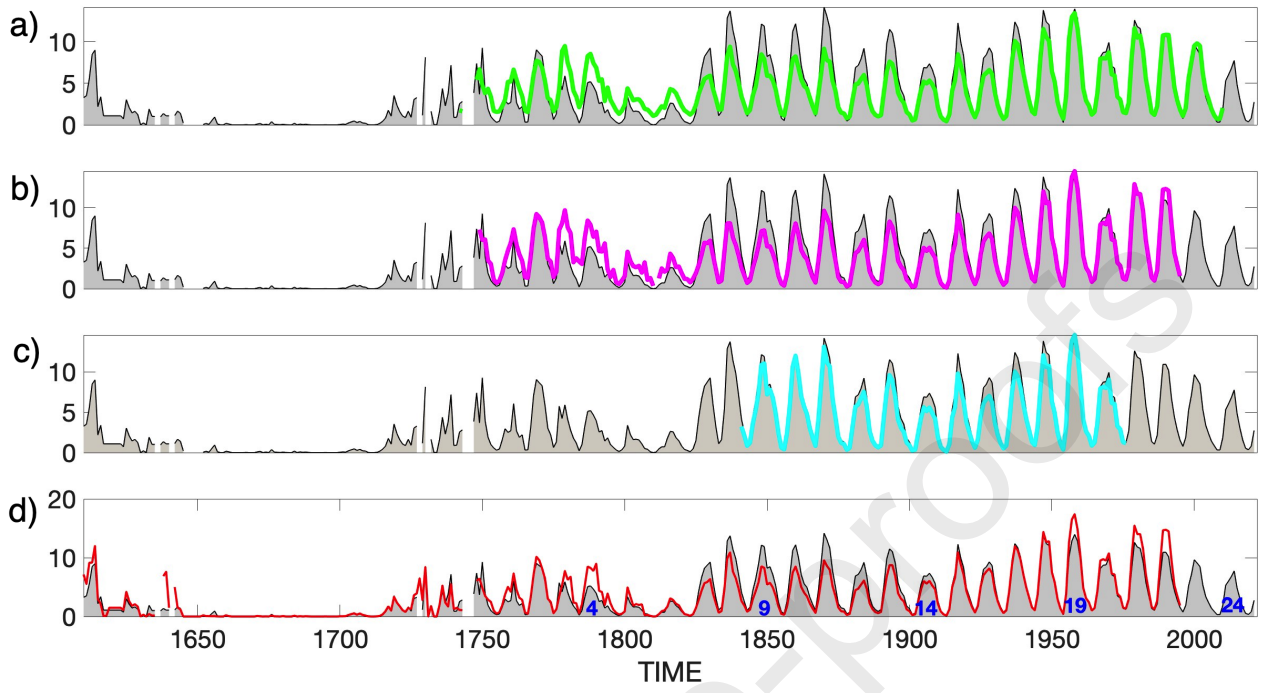

Figure 10. Comparison between our new and calibrated annual GSN reconstruction represented by shaded area and a black line and: (a) GSN reconstruction of Chatzistergos et al. (2017) (green line), (b) GSN reconstruction of Usoskin et al. (2016) (pink line), (c) GSN reconstruction of Cliver and Ling (2016) (blue line), and (d) reconstruction of GSN by Hoyt and Schatten (1998) (red line).

3.7. Wavelet Analysis

The temporal comparison of the variations of the new daily GSN reconstructed using the inter-calibration algorithms with other GSN reconstructions in Sections 3.2, 3.3 and 3.4 shows the novelty of our new results. However, it is also necessary to find the spectral contents or periodicities contained in the new GSN record and assess the information relative to other recent GSN reconstructions.

Figure 11 shows the full results of the wavelet analysis of the newly reconstructed daily HVP-GSN record based on our inter-calibration algorithm (Equation 1) from 1610 to 2022. The global wavelet spectrum shows periodicities greater than the 95% confidence level for 119.8 and 10.9 years. The periodicities detected with less than the 95% confidence level are 58.4, 30.9, 20.6, 5.5, 1.2 years.

The periodicity of 119.8 ± 20 years within the uncertainty can be identified to be the periodicity of 120 years. The positive and negative phases of the 120-year periodicity are related to the secular maxima and minima of solar activity as detectable from GSN records, respectively (Velasco Herrera, Mendoza, and Velasco Herrera, 2015; Nagovitsyn and Osipova, 2021; Velasco Herrera, Soon and Legates, 2021; Velasco Herrera et al., 2022a). This periodicity is very stable in isotopes cosmogenic and is present throughout the Holocene (see e.g., Soon et al., 2014).

The periodicity of 58.4±10 years, within the broad uncertainty or even a true indeterminacy of estimates, could be the periodicity of 60 years. Such periodicity has been identified as the Yoshimura-Gleissberg cycle (see, e.g. Soon et al., 2014, for discussion and references) and has been proposed that this periodicity is related to the solar system barycenter, i.e. with the inertial motions of the Sun around the solar system center of mass (Cionco and Pavlov, 2018). So this periodicity can be of gravitational origin that has, in turn, been speculated to modulate the solar magnetic field (Stefani, Giesecke, and Weier, 2019). Recently, Nagovitsyn, Osipova,

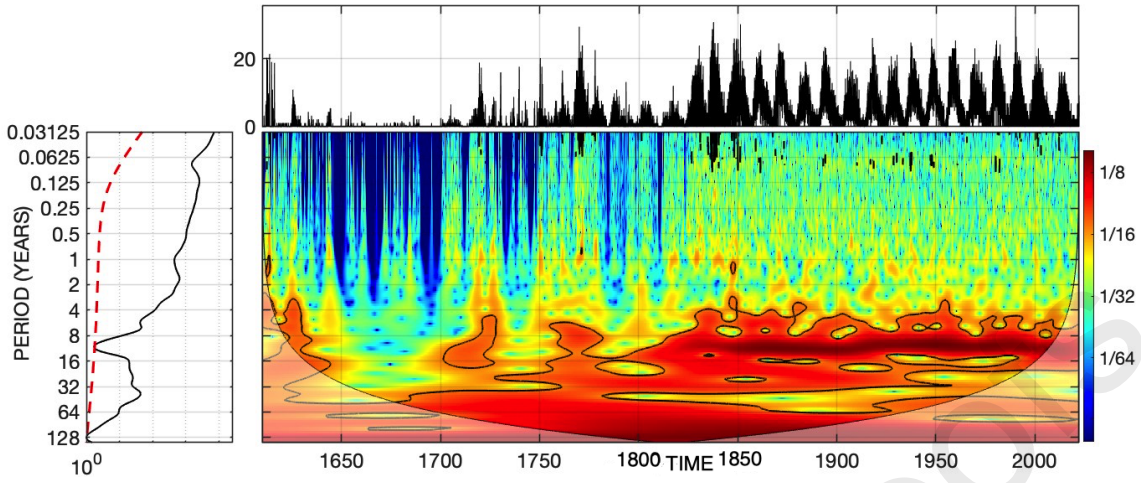

Figure 11. Time-frequency wavelet results of the new daily group sunspot numbers from 1610-2021 reconstructed by our objective calibration algorithm. The full range of periodicities was searched and studied but we focus the discussion mainly for periods from 1 year to 120 years in the main text. The time-frequency regions with wavelet spectral power detection above 95% confidence level are marked with thin black contours. The lower panel shows the calculated wavelet Power Spectral Density (PSD) in normalized units adopting the red-green-blue color scales. The Cone Of Influence (COI,"U"-shaped curve with shaded outer zones) shows the possible edge effects in the PSD. The global time-averaged spectrum is presented in the left panel with the red dashed line representing the 95% confidence level.

and Nagovitsyna (2021) noted a potentially distinct 50-year cycle in their carefully constructed 145-year long records of so-called "generative" indices of sunspot activity. Those authors found that this 50-year oscillation has a similar phase variation with the north-south asymmetry indices as well, thus hinting at a new secular cycle different from the traditional Gleissberg cycle of about 88-year.

The periodicity of 30.9 ± 5 years is the 30-year solar periodicity has been reported in the analysis of cosmic ray activity records by Perez-Peraza et al. (2012). Nagovitsyn, Osipova, and Nagovitsyna (2021) reported and discussed a weak 30-year-like cycle in their new sunspot activity indices as well as in the study of sunspot area records with different sizes. We wish to emphasize that this solar activity period should not yet be directly recognized to be connected to the so-called "Bruckner-Egeson-Lockyer" climatic cycles of 30-40 years known in the literature (see e.g., Clough, 1905; Halberg et al., 2010). The 22-year periodicity is indeed the solar magnetic polarity cycle (the Hale cycle). The 10.9 ± 3-year periodicity, with a broad range of indeterminacy, is the Schwabe solar cycle (Schwabe, 1844).

The periodicity of 5.5 ± 1 years is the 5.5-year periodicity provides individual energetic and geometric information for each solar cycle (period, phase, amplitude, duration, etc). This periodicity has also been recognized as a subharmonic of the 11-year solar cycle (Polygiannakis, Preka-Papadema and Moussas, 2003; Velasco Herrera, Soon and Legates, 2021). Furthermore this important periodicity has been reported in different solar indices as historical aurora records, SSN, ^{10}Be cosmogenic isotope, polar-facula activity records, GSN, and Solar Flare Index (see e.g., Silverman, 1992; Usoskin et al., 2006; Kollath and Olah, 2009; Le Mouël, Lopes, and Courtillot, 2019, 2020; Velasco Herrera, Soon and Legates, 2021; Velasco Herrera et al., 2022b)

The quasi-biennial oscillation (QBO) in solar activity are periodicities roughly between 0.6 and 4 yr (Benevolenskaya, 2000; Howe et al., 2000; Mendoza, Velasco, and Valdés-Galicia, 2006; Obridko and Shelting, 2007; Valdés-Galicia and Velasco Herrera, 2008; Fletcher et al., 2010; Bazilevskaya et al., 2014, 2016; Kiss, Gyenge and Erdélyi, 2018; Velasco Herrera et al., 2018). Although it should be clarified that biennial means two years, so it is not clear why the QBO are extended to periodicities up to four years. Also, previous researchers have suggested that these periodicities can be plausibly associated with various solar dynamo processes. In exploring QBO further, the periodicities between 1 and 2 years are further classified as the mid-term periodicities (MTP). These

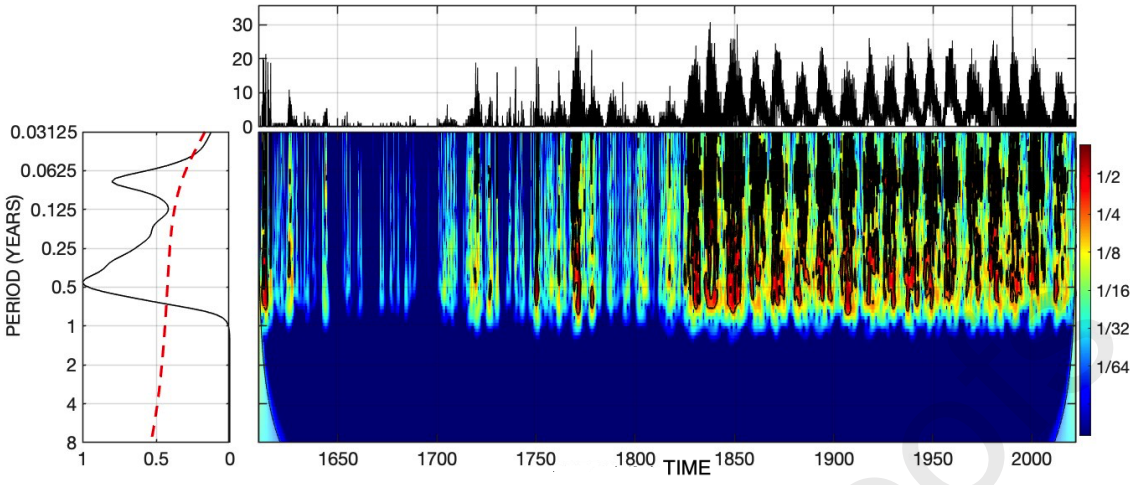

Figure 12. Time-frequency wavelet results of the new daily group sunspot numbers for periodicities less than one year from 1610-2022.

MTP periodicities have been reported in coronal hole area, long duration X-ray solar emissions, solar wind velocity, and galactic cosmic ray intensity (see e.g., Antalová, 1994; Valdés-Galicia, Otaola, and Pérez-Enríquez, 1996; Mendoza, Velasco, and Valdés-Galicia, 2006; Valdés-Galicia and Velasco Herrera, 2008). Periodicities of less than one year will be analyzed and discussed in another work.

3.8. The study of periodicities shorter than one year and differential solar rotation

The wavelet spectral analysis of the daily GSN data from Figure 11 reveals that the 11-year and 119-year solar cycle periodicities exhibit the highest spectral power. To highlight periodicities shorter than 11 years, especially those less than 1 year, we filter out or remove all periodicities longer than 1 year as previously shown in Figure 11. The global spectrum of the daily GSN shows that for periodicities less than one year, we can identify periods 3.5, 5.4, 9.8, 27.8, 66.1, 117.8, and 160.5 days. The results are displayed in Figure 12.

The periodicity of 160.5 days, with the full range of uncertainty and indeterminacy, can vary between 150 and 170 days. This periodicity is reported convincingly for the first time by Rieger et al. (1984) based on the statistical data of hard X-ray solar flares. Furthermore, Rieger reports a peculiarity in the temporal distribution of these high-energy events of 154 days, since these events are not randomly distributed in time. Rather, they tend to occur in clusters with an average spacing of about 154 days. This type of spatial distribution is a characteristic of abrupt physical processes (see, e.g., Velasco Herrera et al., 2018, 2022c,d)

Our study of the newly reconstructed daily GSNs showed that before, during and after the Maunder minimum the Sun's rotational periodicity has not changed significantly from 27 days. The effect of the solar differential rotation has effects on the solar magnetic field and has been measured from the photosphere to the corona in different solar indices and various values have been reported between 25 and 31 days that show the different solar latitudinal speeds (Kane, Vats and Sawant, 2001; Kane, 2002a,b, Velasco Herrera et al. 2022a). These results possibly suggest that there is, empirically, a synchronization of the modulation of the solar rotation among different solar layers.

The solar periodicities less than 20 days reported in this work, that is, periodicities of 9.8, 5.4, and 3.5 days, most likely show certain behavior of the solar photosphere or the internal behavior and interaction processes of the solar magnetic field. Possibly these periodicities maybe a key to probe what happens below the photosphere, as well as to analyze the spatio-temporal variations of magnetic fields within the solar convection zone. However, these smaller-scale magnetic fields have not yet been directly observed

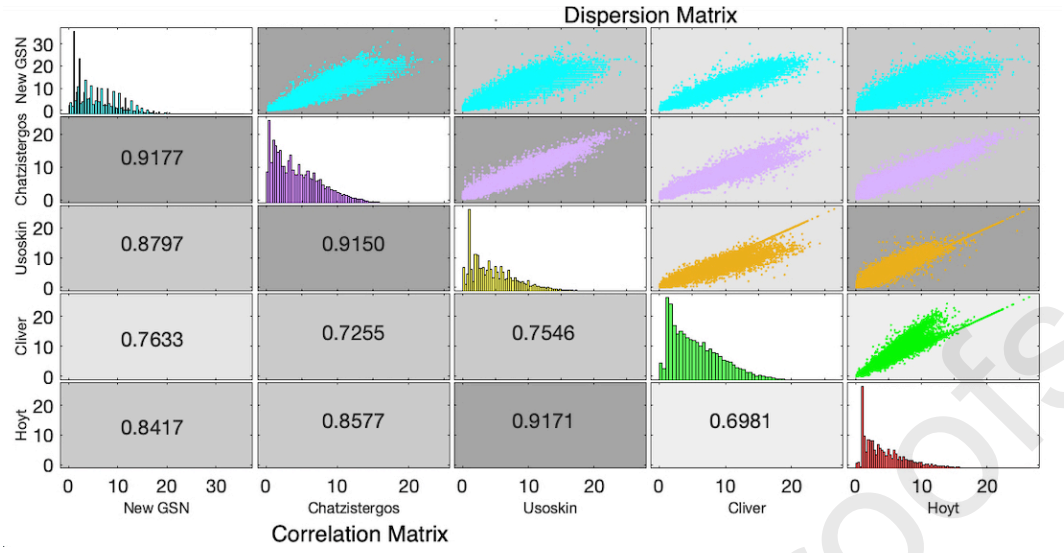

Figure 13. Correlation and dispersion matrix. The dispersion matrix of the various GSN reconstructions (i.e., studied and compared in Figures 8, 9 and 10) is depicted above the diagonal line of the full matrix. Below the diagonal line, we present the correlation coefficient values for the different combinations of the five GSN reconstructions analyzed in this study. The diagonal elements represent histograms for each of the GSN reconstructions examined in this study.

and measured (Švanda et al., 2016; Tlatov, 2022a). Also, the periodicities of 5.4 and 3.5 days could be related to the disintegration of the sunspot groups in a quasi-regular manner, i.e., with the decay of the magnetic fields of the active region of the sunspot group, because they represent the evolution of the emerged magnetic field complexes (Muraközy, 2020, 2021, 2022). Therefore, more analysis is required to confirm or rule out these plausible physical phenomena but the tentative interpretation emphasizes the need for the high temporal resolutions of the solar and sunspot activity datasets.

3.9. Correlation and dispersion analysis

In a scatter plot, such as the ones shown in the elements above the diagonal line of the matrix represented in Figure 13, the patterns can take the form of a straight line, an ellipse, or another shape (Green, 1976). These representations provide essential information regarding the relationship between two GSN reconstructions. When a scatter plot exhibits a straight line that fits the scattered points, it implies a strong linear relationship between the two GSN records. The slope of the line reflects the magnitude of the relationship. In the case of an narrower ellipse in a scatter plot, it signifies a strong correlation, while if this ellipse is wide, it indicates a more uniform correlation between both variables (Green, 1976).

Figure 13 also displays the scatter matrix among the different GSN reconstructions analyzed in this study. These graphs are situated above the diagonal line of the matrix. In cyan color, the various scatter plots between our new GSN reconstruction and the four previously reported GSN datasets are depicted. It can be observed that, in general, these plots assume an elliptical form, suggesting strong and homogeneous dispersion.

Furthermore, on average, the correlation coefficients between our new GSN reconstruction and the four GSN records, shown below the diagonal line of the matrix, are higher when compared to the correlations among the remaining GSN reconstructions. We wish to highlight peculiar cases as well. The dispersion between the Usoskin et al. (2016) and Cliver and Ling (2016) reconstructions, concerning the Hoyt and Schatten (1998) reconstruction, forms a straight line for GSN values greater than 15, indicating a strong linear relationship among these three reconstructions. Additionally, in the diagonal elements of the matrix presented in Figure 13, histograms for each of the GSN reconstructions analyzed in this study are represented.

Having conducted a global comprehensive analysis that considered both dispersion and correlation between our new GSN

reconstruction and four previously reported GSN reconstructions, we are now ready to delve into a localized examination using cross-wavelet analysis. This approach allows us to explore next a more localized investigation of the distinctions and similarities between two GSN time series, specifically, to exclusively investigate the covariance between our new GSN reconstruction and each of the four GSN series under comparative scrutiny in this study.

3.10. Multi-Cross and Cross Wavelet Analyses

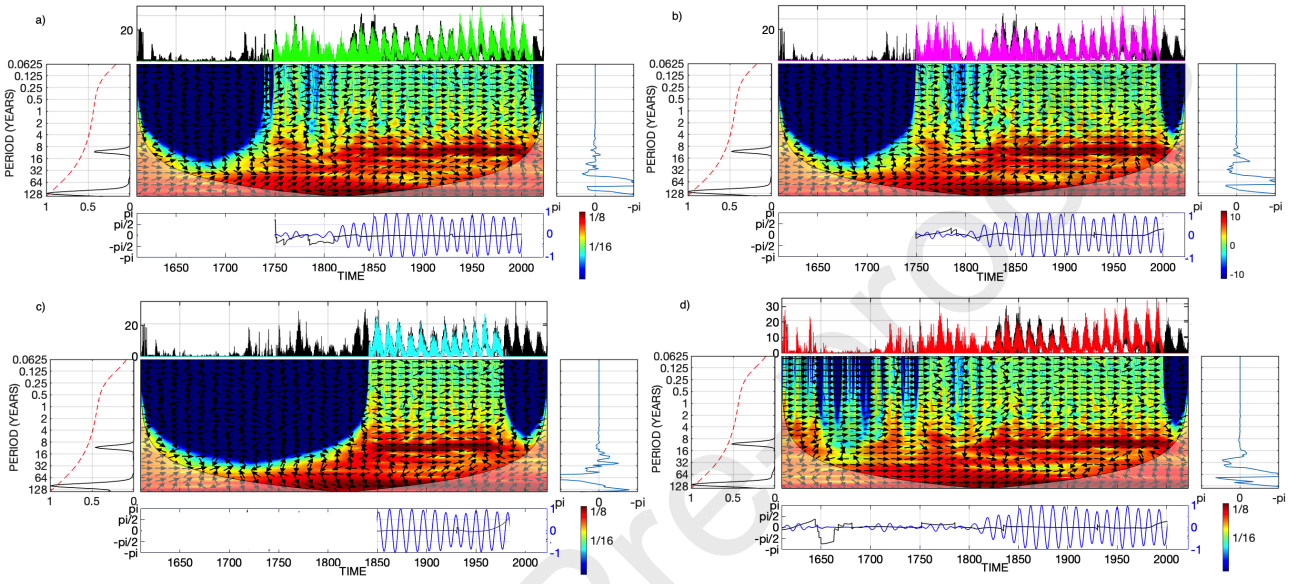

Figure 14. The time-frequency gapped cross-wavelet spectrum between our newly developed group sunspot number (GSN) reconstruction and four other distinct GSN records. In the upper panel, the GSN time series is depicted and analyzed within this study. The new GSN reconstruction is represented by the black line, while the analized reconstructions are as follows: (a) GSN reconstruction of Chatzistergos et al. (2017) in green line, (b) GSN reconstruction of Usoskin et al. (2016) in pink line, (c) GSN reconstruction of Cliver and Ling (2016) in blue line, and (d) reconstruction of GSN by Hoyt and Schatten (1998) in red line. The left panel shows the global cross spectrum. The center panel shows the local wavelet spectrum. The black arrows indicate the relative phase between the time series of the upper panel The orientations from left to right (→) and from right to left (←) signify linear, in-phase, and antiphase synchronizations at specific frequencies between these phenomena. Any other orientation suggests a complex, non-linear covariance or synchronization relationship. The right panel shows the global phase. The lower panel shows the local phase in black line and the oscillation for the 11-yr periodicity of the solar cycle between the time series of the upper panel.

In addition to the straight time series comparisons presented in Section 3.3, which encompasses four distinct GSN reconstructions, we recognize the necessity of a spectral analysis to reveal intricate patterns and covariances among these time series and our new innovative GSN reconstruction. Traditional spectral analysis encounters two primary challenges: firstly, the presence of data gaps across all time series at varying timescales, and secondly, conventional cross or coherent spectral methods lack the capacity to simultaneously analyze the total of five GSN time series records investigated in this study.

Existing methodologies predominantly operate on pairwise time series. That is why we use the gapped cross wavelet (see Soon et al., 2019, for more details on the methodology). In Figure 14a, we present the result of the cross wavelet analysis between the new GSN reconstruction, depicted by the black line, and the reconstruction by Chatzistergos et al. (2017), shown by green line. In the central panel, it becomes evident that the relative phases between these two time series, for periodicities shorter than the 11-year solar cycle, exhibit an average orientation from left to right, this mean that both GSNs show a linear co-variation. Also, this spectral behavior indicates that both GSN reconstructions capture solar variations equivalently. Hence, the differences in amplitudes depicted in Figure 8a between these same GSN reconstructions manifest as arrows pointing in different directions.

Notably, between 1750 and 1800, there is a discrepancy in arrow directions, possibly attributable to the limited data utilized in Chatzistergos et al. (2017) reconstruction.

Furthermore, for periodicities longer than the solar cycle, some arrows deviate from the left-to-right direction. This discrepancy arises from Chatzistergos et al. (2017) reconstruction lacking GSN values between 1610 and 1750. Additionally, between 1750 and 1800, substantial differences emerge between both GSN reconstructions, potentially due to a smaller dataset used and original GSN data gaps. These differences are illustrated in the lower panel, which presents the relative phase of the solar cycle between these two reconstructions (depicted by the black line) alongside the oscillation of the solar cycle (depicted by the blue line).

In the right panel of Figure 14a, the global phase relationship between these two GSN reconstructions is displayed, while the left panel focuses on the specific periodicities of the solar cycle and the secular solar periodicity. It is conceivable that these two GSN periodicities are spectrally equivalent between 1800 and 2000. However, due to Chatzistergos et al. (2017) methodology failing to reconstruct GSN data between 1610 and 1750, it is not possible to strictly compare the covariance between these two GSN reconstructions.

The Figure 14b shows the result of the cross wavelet analysis between the new GSN reconstruction and Usoskin et al. (2016)'s reconstruction in pink line. Due to the similarity between the methodologies used by Chatzistergos et al. (2017) and Usoskin et al. (2016), the central panel of Figure 14b exhibits a similarity in spectral behavior, thus the result is very similar to what was found in Figure 14a.

Figure 14c displays the outcome of the cross-wavelet analysis between the new GSN reconstruction and Cliver and Ling (2016)s reconstruction in blue line. The relative phases exhibit a striking resemblance to the findings in Figure 14a-b. This consistency underscores the robustness of our results and strengthens the evidence supporting the validity of our analysis.

Finally, Figure 14d illustrates the covariance between the new GSN reconstruction and the pioneering GSN reconstruction carried out by Hoyt and Schatten (1998) in red line. The relative phases reveal that these two reconstructions are not identical, as not all arrows align from left to right; they exhibit different orientations, primarily due to distinct methodologies employed. The most significant disparity between these reconstructions is observed at the onset of the Maunder Minimum.

The present spectral analysis here highlights that the primary differences among the various GSN reconstructions are previously concentrated in the discussion of differing GSN amplitudes. However, there is a noticeable lack of discussion regarding spectral differences and similarities. Thus, our new cross-wavelet results demonstrate the spectral equivalence between our GSN reconstruction and the four other independent GSN reconstructions. Notably though, three out of these four GSN records fail to reconstruct GSN activity during the Maunder Minimum using their proposed methodologies.

The analysis of dispersion, correlation, and cross-wavelet reveals that the new GSN reconstruction exhibits the highest covariance, dispersion, and correlation with the four analyzed GSN reconstructions. However, this does not necessarily imply a consistent pattern among all GSN reconstructions, as is partially evident in the dispersion and correlation matrix. To shed light on this from a spectral content perspective, we will now conduct a spectral analysis of the five reconstructed GSN datasets simultaneously using a novel spectral analysis approach. We apply the multi-time series cross wavelet approaches tailored for gapped time series to scrutinize the concurrent covariances among the aforementioned five GSN time series (see e.g., Soon et al., 2014; Velasco Herrera et al., 2017, for more details on the method).

Figure 15 shows the multi-cross wavelet analysis between the five time series analyzed in this study that are shown in the upper panel with different colors. The multi-cross wavelet spectrum shows the following periodicities that exist simultaneously and commonly in all five GSN reconstructions: 1.2, 2, 3.4, 5.47, 10.8, 19.4, 56.5, and 115.7 years. This result means that all

GSNs are equivalent although there are substantial differences that we will discuss below. Of the 8 covariant periodicities, two periodicities are detected with more than or equal to the 95% confidence level, which are the periods of 115.7 and 10.8 years, respectively. The remaining six periodicities have been detected below the 95% significance level. However, this does not mean that these periodicities are spurious or fictitious, but that their spectral power is relatively lower than the spectral power of the 10.8 and 115.7 year periodicities. This is very important to emphasize because a global wavelet spectrum is often confused with the interpretation for the Fourier spectral analysis result (see, e.g., Torrence and Compo, 1998; Soon et al., 2019, for more details on the method). The physical significance of these six periodicities has been discussed above when we have analyzed them for our new GSN reconstruction from 1610-2021.

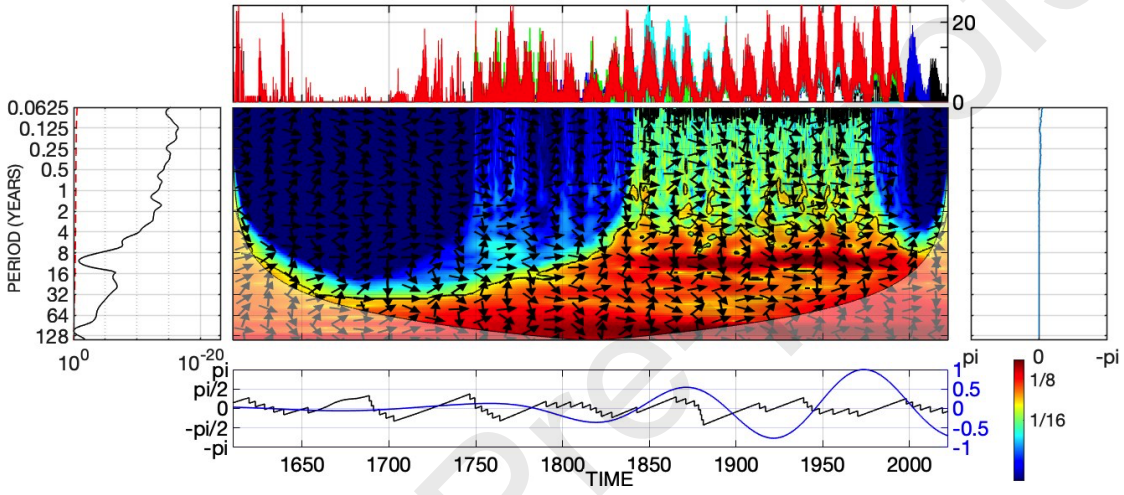

Figure 15. Time-frequency gapped multi-cross wavelet spectrum of the covariations between five different group sunspot numbers reconstructions analyzed from 1610 to 2021. The upper panel shows the five GSN time series analyzed in this work with different colors: (a) GSN reconstruction of Chatzistergos et al. (2017) in green, (b) GSN reconstruction of Usoskin et al. (2016) in pink, (c) GSN reconstruction of Cliver and Ling (2016) in blue, (d) reconstruction of GSN by Hoyt and Schatten (1998) in red, and (e) the new HVP GSN reconstruction in black. The central panel shows the gWTC power adopting the red-green–blue color scales. The power in red color indicates highest (perfect)-degree of frequency covariance (synchronization) between all GNS time series. The power in blue color indicates the minimum or null covariance between all GSN-record. The black arrows indicate the relative phase of the synchronization. The orientations from left to right (→) and from right to left (←) indicate that there is a linear, in-phase and antiphase, synchronization at a certain frequency between these phenomena. Any other orientation means that there is a complex, non-linear covariance or synchronization. The left-hand panel shows the global gapped time-averaged wavelet coherence spectrum with the red dashed line representing the 95 per cent significance level. The panel on the right shows the global gapped frequency-averaged wavelet cross spectrum. The bottom panel shows the coherence function of 120-yr period in blue continuous line and the instantaneous phase relative for this same period in black line (see Velasco Herrera et al., 2017, for more details on the method).

The evolution of the covariance is shown in the central panel of Figure 15. We can see the difference with the wavelet spectral analysis of our reconstructed GSN shown in Figure 11. Due to the gaps in all GSNs, the covariance is near zero or exactly zero during the Maunder minimum and very low for the 1750 to 1850 interval, so for the remaining reconstructed GSNs, although they have a daily resolution, have too many gaps between 1750 and 1850 to yield meaningful spectral results. These gaps result in zero or very low covariance from 1610 to 1850 for the periodicities under 30 years. Within this time interval, the periodicities less than 30 years, the spectral power is minimal or near zero and therefore only shades of blue with the lowest spectral powers are indicated.

This result shows that it is not enough to have some daily GSN data, but it is necessary to use all the GSN data reported by the different observers in order to minimize the gaps between the observed GSNs. Using only some selected observers with some GSN reported from the point of view of spectral analysis is not correct because these limited techniques and methodologies result in a loss of information for periodicities of less than 30 years. This implies from the point of view of optimization and signal theory that instead of having some daily data with large gaps it is equivalent to having 30-year multi-decade averages for the period from 1610 to 1850. These data gaps result in a loss of information on solar magnetic activity variations.

Figure 15 also clearly shows the difference of all methodologies used in GSN reconstructions with our objective calibration algorithm. During the 1850 to 1950 interval when there are sufficiently dense data series, a mean covariance is observed between all the time series, which means that there are fewer gaps in the time series and because there is no update in the different GSN time series after 1990 again. There is a very low or nearly zero covariance for periodicities less than 8 years.

There is a very high covariance for the periodicity of the 11-yr-like sunspot cycle and for the secular 120-yr solar periodicity from 1750 to 2021. The instantaneous phase (represented by the arrows in the central panel) clearly shows the differences between the different reconstructions due to the individual methodologies used. This result can be seen in the global phase found in the panel on the right. The fact that the blue line is centered at zero does not mean that all the GSNs are synchronized, but rather that the instantaneous phases are in all possible directions and that is why the average is almost zero because of nearly total self-cancellation. This multi-cross wavelet analysis between all the reconstructed GSNs clearly shows that from the spectral point of view all previously reported GSNs lack solar magnetic information from 1750 to 1850 for periods less than 30 years. In contrast our newly reconstructed GSN using all observers with all their GSN data shows the robustness and validity of our new GSN database as well as its reconstruction using our objective calibration algorithm (see e.g., result presented in Figure 11).

The loss of solar magnetic information in the different GSN time series clearly shows the need to gather as much information as possible in order to have a more complete analysis of the solar magnetic activity variation since the Maunder minimum.

4. Comparison between GSN and SSN

In section 3, different comparisons were made between the new GSN reconstruction and other GSN reconstructions. In this section a daily comparison will be made between the GSN and the Sunspot Number, SSN (version 2.0) from the Sunspot Index and Long-term Solar Observations (SILSO) database hosted at the Royal Observatory of Belgium. The GSN record remains to this day the longest direct observational time series of the sun. The daily record of SSN begins in 1818 and is the second direct observational record of the sun. The purchase will be made from 1818 to 2022 in order to have the complete years. Of the possible 74875 data, our GSN reconstruction contains 63778 data points, while the SSN records have 60230 data values. Thus our GSN record has 5% more data than the SSN record offerred by SILSO.

Figure 16 shows the result of the comparison between the new GSN reconstruction (cyan dotted line) and the SSN v2.0 record (black line). It can be seen that in general there is a good overall agreement in terms of sunspot cycle activity shapes from solar Cycle 7 to solar Cycle 24. Some differences can be seen in the maxima for solar Cycles 19, 21, and 22.

5. Summary and Conclusion

This study proposes a new daily, monthly and yearly reconstruction GSN records from 1610 – 2021 applying a novel method of inter-calibration algorithm of the HVP-GSN records based on the Pulkovo Observatory as reference observer. This new HVP-GSN dataset can be and will be actively and continuously updated according to the needs and interests of all solar researchers. We are also able to assess and confirm the novel and reliability of the result of our daily GSN reconstructions by detailed comparison with four other previous GSN reconstructions. Another very important bonus result from this paper is the straightforward update of the original Hoyt and Schatten (1998) GSN record from 1610 to 2021 with the 1996-2021 interval fulfilled by the Pulkovo Observatory GSN records.

Indeed, our new daily, monthly, and annual HVP GSN reconstructions compare reasonably well with three other recent GSN reconstructions by Cliver and Ling (2016); Usoskin et al. (2016); Chatzistergos et al. (2017). More importantly, our new HVP-GSN

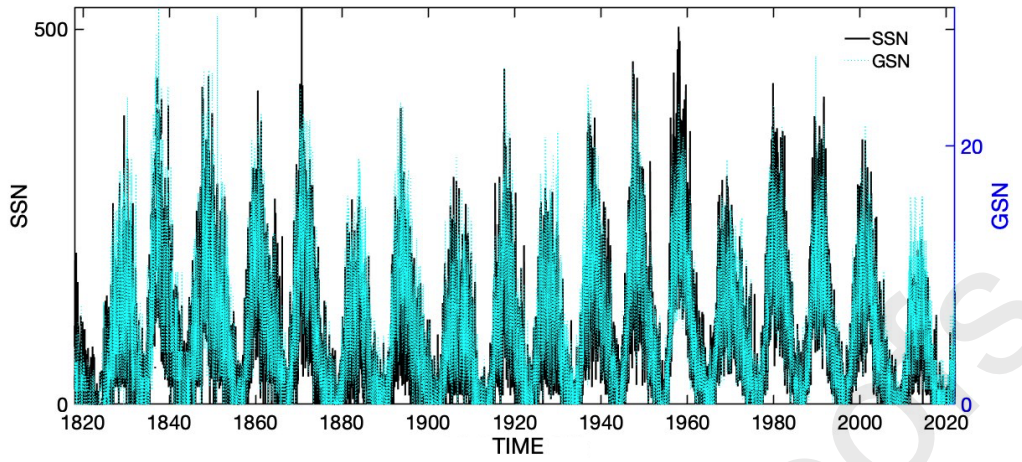

Figure 16. Comparison between our daily GSN reconstruction (cyan dotted line) and the daily SSN version 2.0 (black line) from 1818 to 2022.

record also compares relatively well with the calibrated Hoyt and Schatten (1998) GSN record both from the direct time series comparison as well as from spectral content perspectives.

We would like to highlight a key aspect of our calibration algorithm (Equation 1), its ability to effectively handle gapped time series data, particularly during the Maunder minimum. Furthermore, our objective algorithm is a viable alternative to classical methods of compositing sunspot activity time series such as backbone, cross-calibrating the raw count records, and daisy-chaining of k–factors. This is mainly because it performs an optimization instead of invoking and assuming arbitrary criteria in the process of in-filling any data gaps and so on.

Also, we have performed a spectral analysis of our newly reconstructed GSN with the objective inter-calibration algorithm which uses all observers with all their reported data, so our methodology is inclusive and does not exclude any solar magnetic information. We have carried out the time-frequency analyses of the new daily reconstructed GSN records. We report the detection of periodicities of 119.8 (as the secular maxima and minima of solar activity that can be resolved within GSN records), 58.4 (Yoshimura-Gleissberg cycle), 30.9, 20.6 (Hale cycle), 10.9 (Schwabe cycle), 5.5 (Quasi-Quinquennial cycle), and 1.2 years. The wavelet spectral analysis shows that our new database is solid, novel and has all the solar magnetic information. The gaps that our reconstructed GSN has show some loss of information for periodicities of less than four years during some small time intervals. These results contrast with the different GSN reconstructions previously reported and analyzed in this work.

Regarding the reported periodicities with the wavelet analysis of our new GSN reconstruction, we want to highlight that all the reported periodicities have been presented and published in previous scientific works (e.g. Polygiannakis, Preka-Papadema and Moussas, 2003; Nagovitsyn, 2007). This fact means that the new methodology applied to the new GSN database reproduces nearly all of the previously reported, claimed or established sunspot periodicities. In this respect, we wish to highlight explicitly that our working hypothesis is that all periodicities detected with the wavelet analisys are present even during the Maunder Minimum, particularly the periodicities of the magnetic cycle (Hale cycle), solar cycle of 11 years (Schwabe cycle), the quasi-biennial oscillation (QBO), and the periodicities shorter than one year such as the Rieger cycle and periodicity of the solar differential rotation.

Our main hypothesis is based on the fact that there are no physical reasons to presuppose that the physical properties in the solar cycles during the Maunder minimum must be different such that the solar dynamo must be operating in a different

physical reality for solar activity when not in the Maunder minimum phase. The main difference between these solar cycles during the Maunder minimum and non-Maunder minimum intervals must be: 1) the amplitude of the oscillations or periodicities, and 2) some studies suggest that these periodicities may not exist likely due to the artefacts from the lack of data. We highlighted these points because there are no known theoretical model nor understanding to demonstrate the absence or disappearance of those short-term periodicities.

The multi-cross wavelet analysis, however, indicates a loss of information for periodicities of less than 30 years especially for the time interval from 1750 to 1850 in the different GSN records analyzed in this work. We conclude that there is a loss of information for well over a century of solar observations from 1610 to 1860 in some of the previous GSN reconstructions. Due to the lack of updating of these earlier GSN records, our analysis also indicates a loss of information from 1990 to 2022 for periodicities less than 8 years. This surprising hint clearly argues for the need to complete the solar information of sunspots from 1610 to 1850 and from 1990 to 2022. That is why our new daily HVP GSN reconstruction meets this need by containing the smallest gaps and the smallest possible losses of solar information since the Maunder minimum. In addition, this paper also has been able to provide the important update of the original Hoyt and Schatten (1998) GSN records from 1610 till 2021.

Acknowledgements

We thank the anonymous reviewers for their critical reviews which have led to improvements of the current manuscript. We are also very grateful to Douglas Hoyt for his many selfless discussions on historical sunspot observations and the reconstruction of GSN. Velasco Herrera acknowledges the support from CONACyT-180148 and the support from PAPIIT-IT102420 grants. W. Soon's work was partially supported by CERES and he acknowledges Professor Laszlo Szarka and the EPSS of Hungary for the honorific title and position. Andrey Tlatov acknowledges project "Science" by the Ministry of Science and Higher Education of the Russian Federation under the contract 075-03-2022-119/1.

Data Availability and Supplementary Material

The new HVP GSN data as well as the updates to the original HS98 GSN record from this study are available from the corresponding author. The update of the original Hoyt and Schatten (1998) GSN record with revision from Vaquero et al. (2016) database and with update from the Pulkovo Observatory determination of GSNs as well as all the reconstructed HVP-GSNs in daily, monthly and annual resolutions are also available at:

1. https://drive.google.com/drive/folders/1srjF065iuhJkmgvITxg5aUqP7Y1PG3tL?usp=sharing
2. https://www.ceres-science.com/publications

References

Antalová, A.: 1994, Periodicities of the LDE-type flare occurrence (1969–1992). *Adv. Space Res.*, **14**, 721. https://doi.org/10.1016/0273-1177(94)90533-9

Baranyi, T., Győri, L., Ludmány, A.:2016, On-line Tools for Solar Data Compiled at the Debrecen Observatory and Their Extensions with the Greenwich Sunspot Data. *Solar Phys.*, **291**, 3081. https://doi.org/10.1007/s11207-016-0930-1

Bayes, T., 1763, An essay towards solving a problem in the doctrine of chances. *Philosophical Transactions of the Royal Society of London* **53**, 370.

Bazilevskaya, G., Broomhall, A.M., Elsworth, Y., Nakariakov, V.M.: 2014, A Combined Analysis of the Observational Aspects of the Quasi-biennial Oscillation in Solar Magnetic Activity. *Space Sci. Rev.*, **186**, 359.

Bazilevskaya, G., Kalinin, M.S., Krainev, M.B., Makhmutov, V.S., Svirzhevskaya, A.K., Svirzhevsky, N.S., Stozhkov, Y.I.: 2016, On the relationship between quasi-biennial variations of solar activity, the heliospheric magnetic field and cosmic rays. *Cosm. Res.*, **54**, 171.

Beer, J., Tobias, S., Weiss, N.: 1998, An active Sun throughout the Maunder Minimum. *Solar Phys.*, **181**, 237.

Benevolenskaya, E.E.: 2000, A mechanism of helicity variations on the Sun. *Solar Phys.*, **191**, 227. https://doi.org/10.1023/A:1005211501835

Brehm, N., Bayliss, A., Christl, M., Synal, H.-A., Adolphi, F., Beer, J., Kromer, B., Muscheler, R., Solanki, S.K., Usoskin, I., Bleicher, N., Bollhalder, S., Tyers, C., Wacker, L.: 2021, Eleven-year solar cycles over the last millennium revealed by radiocarbon in tree rings. *Nature Geosci.*, **14**, 10.

Brogan, W.L.: 1991, Modern Control Theory. *Prentice-Hall International Limited, London UK*, **202**, 309.

Brun, A.S., Strugarek, A., Noraz, Q., Perri, B., Varela, J., Augustsson, K., Charbonneau, P., Toomre, J.: 2022, Powering Stellar Magnetism: Energy Transfers in Cyclic Dynamos of Sun-like Stars, *Astrophys. J.*, **926**, #21.

Bubnicki, Z.: 2005, Modern Control Theory. *Springer-Verlag Berlin Heidelberg, Germany* **421**.

Buffon.: 1733, Geometrie. *Histoire de l'Académie royale des sciences* **43**.

Camporeale, E.: 2019, The Challenge of Machine Learning in Space Weather: Nowcasting and Forecasting. *Space Weather*, **17**, 1166.

Camporeale, E., Johnson, J., Wing, S.: 2018. Machine Learning Techniques for Space Weather, *Elsevier*.

Cappellotto, L., Orgeira, M.J., Velasco Herrera, V.M., Cionco, R.G.: 2022, Multivariable statistical analysis between geomagnetic eld, climate, and orbital periodicities over the last 500 KYR, and their relationships during the last interglacial *Global Planet Change*, **213**, 1166. https://doi.org/10.1016/j.gloplacha.2022.103836

Carrasco,V.M.S., García-Romero, J.M., Vaquero, J.M., Rodríguez, P.G., Foukal, P., Gallego, M.C., Lefevre, L.: 2018, The Umbra-Penumbra Area Ratio of Sunspots During the Maunder Minimum *Astrophys. J.*, **865**, 88. https://doi.org/10.3847/1538-4357/aad9f6

Carrington, R.C.: 1863, Observations of the spots on the Sun from November 9, 1853 to March 24, 1861 (made at Redhill). *Williams and Norgate, London and Edinburgh*.

Casas, R., Vaquero, J.M., Vazquez, M.: 2006, Solar rotation in the 17th century. *Solar Phys.*, **234**, 379.

Charbonneau, P.: 2020, Dynamo models of the solar cycle *Living Rev. Sol. Phys.* **17(4)**

Chatzistergos, T., Usoskin, I., Kovaltsov, G., Natalie A. Krivova, N., Solanki, S.: 2017, New reconstruction of the sunspot group numbers since 1739 using direct calibration and backbone methods *Astron. Astrophys.* **602**, A69 https://doi.org/10.1051/0004-6361/201630045

Cionco, R.G., Pavlov, D.A.: 2018, Solar barycentric dynamics from a new solar-planetary ephemeris. *Astron. Astrophys.*, **615**, A153.

Clette, F., Svalgaard, L., Vaquero, J., Cliver, E.: 2014, Revisting the sunspot number: A 400-yr perspective on the solar cycle. *Space Sci. Rev.*, **186**, 35.

Clette, F., Lefèvre, L., Chatzistergos, T., Hayakawa, H., Carrasco, V.M.S., Arlt, R., Cliver, E.W., Dudok de Wit, T., Friedli, T.K., Karachik, N., Kopp, G., Lockwood, M., Mathieu, S., Munoz-Jaramillo, A., Owens, M., Pesnell, D., Svalgaard, L., Usoskin, I.G., van Driel-Gestelyi, L., Vaquero, J.M.:2023 Recalibration of the Sunspot-Number: Status Report. *Solar Phys.*, **298**, 44.

Cliver, E.W., Ling, A.G.:2016 The Discontinuity Circa 1885 in the Group Sunspot Number, *Solar Phys.*, **291**, 2763.

Clough, H.W.: 1905, Synchronous Variations in Solar and Terrestrial Phenomena. *Astrophys. J.*, **22**, 42.

Connolly, R., Soon W., Connolly, M., Baliunas, S., Berglund, J., Butler, C.J., Cionco, R.G., Elias, A.G., Fedorov, V.M., Harde, H., Henry, G.W., Hoyt, D.V., Humlum, O., Legates, D.R., Luning, S., Scafetta, N., Solheim, J.-E., Szarka, L., van Loon, H., Velasco Herrera, V.M., Willson, R.C., Yan, H., Zhang, W.: 2021, How much has the Sun influenced Northern Hemisphere temperature trends? An ongoing debate. *Research in Astron. Astrophys.*, **21**, # 131.

Connolly, R., Soon W., Connolly, M., Baliunas, S., Berglund, J., Butler, C.J., Cionco, R.G., Elias, A.G., Fedorov, V.M., Harde, H., Henry, G.W., Hoyt, D.V., Humlum, O., Legates, D.R., Luning, S., Scafetta, N., Solheim, J.-E., Szarka, L., Velasco Herrera, V.M., Yan, H., Zhang, W.: 2023, Challenges in the detection and attribution of Northern Hemisphere surface temperature trends since 1850. *Research in Astron. Astrophys.*, **23**, 105015. https://doi.org/10.1088/1674-4527/acf18e

Courant, R., Hilbert, D.: 1924, Methoden der mathematischen Physik 1. *Springer, Berlin*, **464**

Courant, R., Hilbert, D.: 1937, Methoden der mathematischen Physik 2. *Springer, Berlin*, **564**

Dineva, E., Pearson, J., Ilyin, I., Verma, M., Diercke, A., Strassmeier, K.G., Denker, C.: 2022, Characterization of chromospheric activity based on Sun-as-a-star spectral and disk-resolved activity indices *Astron. Nach.*, **343**, e223996.

Eddy, J.A.: 1976, The Maunder Minimum: The Reign of Louis XIV appears to have been a time of real anomaly in the behavior of the Sun. *Science*, **192**, 1189.

Eddy, J.A., Gilman, P.A.,Trotter, D.E.: 1976, Solar rotation during the Maunder minimum. *Solar Phys.*, **34**, 235. https://doi.org/10.1007/BF00157550

Fletcher, S.T., Broomhall, A.M., Salabert, D., Basu, S., Chaplin, W.J., Elsworth, Y., Garcia, R.A.: 2010, A Seismic Signature of a Second Dynamo? *Astrophys. J.*, **718**, L19. https://doi.org/10.1088/2041-8205/718/1/L19

Fourier, J.B.J.: 1822, Théorie Analytique de la Chaleur. *Libraires Pour Les Mathématiques, L'Arquitecture Hydraulique et la Marine*,

Frick, P., Baliunas, S.L., Galyagin, D., Sokoloff, D., Soon, W.: 1997, Wavelet analysis of stellar chromospheric activity variations, *Astrophys. J.*, **483**, 426.

Frick, P., Grossman, A., Tchamitchian, P.: 1998, Wavelet analysis of signals with gaps, *Journal of Mathematical Physics*, **39**, 4091.

Galilei, G.: 1613, Istoria e dimostrazioni intorno alle macchie solari e loro accidenti: comprese in tre lettere, *Appresso Giacomo Mascardi* **39**, 55. https://repository.ou.edu/uuid/edeaba71-97d3-5c9c-8865-69be7cc980b6#page/66/mode/2up

Gilman, D. L., Fuglister, F. J., Mitchell, J.: 1963, On the Power Spectrum of "Red Noise". *Journal of the Atmospheric Sciences*, **20**, 182.

Gray, L.J., Beer, J., Geller, M., Haigh, J.D., Lockwood, M., Matthes, K., Cubasch, U., Fleitmann, D., Harrison, R.G., Hood L., Luterbacher, J., Meehl, G.A., Shindell, D., van Geel, B., White, W.: 2010, Solar influences on climate. *Rev. Geophys.*, **48**, RG4001.

Green, P.E.: 1976, Mathematical Tools for Applied Multivariate Analysis. *Academic Press, New York*, 381.

Grossmann, A., Morlet, J.: 1984, Decomposition of Hardy functions into square integrable wavelets of constant shape. *SIAM J. Math. Anal.* , **15**, 723.

Győri, L., Ludmány, A., Baranyi, T.: 2017, Comparative analysis of Debrecen sunspot catalogues. *MNRAS*, **465**, 1259. https://doi.org/10.1093/mnras/stw2667

Halberg, F., Cornelissen, G., Bernhardt, K.-H., Sampson, M., Schwartzkopff, O., Sonntag, D.: 2010, Egeson's (George's) transtridecadal weather cycling and sunspots. *History of Geo- and Space Sciences*, **1**, 49.

Hayakawa, H., Iwahashi, K., Tamazawa, H., Toriumi, S., Shibata, K.: 2018, Iwahashi Zenbei's Sunspot Drawings in 1793 in Japan, *Solar Phys.*, **293**, # 8.

Hayakawa, H., Kuroyanagi, C., Carrasco, V.M.S., Uneme, S., Besser, B.P., Soma, M., Imada, S.: 2021, Sunspot Observations at the Eimmart Observatory and in Its Neighborhood during the Late Maunder Minimum (1681-1718), *Astrophys. J.*, **909**, # 166.

Howe, R., Christensen-Dalsgaard, J., Hill, F., Komm, W., Larsen, R. M., Schou, J., Thompson, M., Toomore, J.: 2000, Dynamic variations at the base of the solar convection zone. *Science*, **287**, 2456. https://doi.org/10.1126/science.287.5462.2456

Hoyt, D., Schatten, K.H.: 1997. **The Role of the Sun in Climate Change**, *Oxford University Press*.

Hoyt, D., Schatten, K.H.: 1998, Group Sunspot Numbers: A New Solar Activity Reconstruction. *Solar Phys.*, **181**, 491.

IPCC: 2021, Climate Change 2021: The Physical Science Basis. *Contribution of Working Group I to the Sixth Assessment Report of the Intergovernmental Panel on Climate Change.* Masson-Delmotte, V., Zhai, P., Pirani, A., Connors, S.L., Pean, C., Berger, S., Caud, N., Chen, Y., Goldfarb, L., Gomis, M.I., Leitzell, K., Lonnoy, E., Matthews, J.B.R., Maycock, T.K., Waterfield, T., Yelekci, O., Yu, R., and Zhou, B. (eds.) (Cambridge Univ. Press, Cambridge, United Kingdom and New York, NY, USA), 2391 pp.

Karachik, N.V., Pevtsov, A.A., Nagovitsyn, Y.A.: 2019, The effect of telescope aperture, scattered light and human vision on early measurements of sunspot and group numbers. *Mon. Not. Roy. Astron. Soc.*, **488**, 3804.

Kiss, T.S., Gyenge, N., Erdélyi, R.: 2018, Quasi-biennial oscillations in the cross-correlation of properties of macrospicules. *Adv. Space Res.*, **61**, 611.

Kollath, Z., Olah, K.: 2009, Multiple and changing cycles of active stars: I. Methods of analysis and application to the solar cycles. *Astron. Astrophys.*, **501**, 695.

https://doi.org/10.1051/0004-6361/200811303
Le Mouël, J.L., Lopes, F., Courtillot, V.: 2019, A Solar Signature in Many Climate Indices. *J. Geophys. Res.*, **124**, 2600. https://doi.org/10.1029/2018JD028939
Le Mouël, J.L., Lopes, F., Courtillot, V.: 2020, Characteristic Time Scales of Decadal to Centennial Changes in Global Surface Temperatures Over the Past 150 Years. *Earth Spa. Sci.*, **7**, e2019EA000671. https://doi.org/10.1029/2019EA000671
Makarov, V.I., Tlatov A.G.: 2000, Polar Magnetic Field Reversals of the Sun in Maunder Minimum. *J. Astrophys. Astr.*, **21**, 193. https://doi.org/10.1007/BF02702389
Maunder, E.W.: 1894, A prolonged sunspot minimum. *Knowledge*, **17**, 173.
Mendoza, B., Velasco, V. M., Valdés-Galicia, J.F.: 2006, Mid-Term Periodicities in the Solar Magnetic Flux. *Solar Phys.*, **233**, 319.
Muraközy, J.: 2020, Study of the Decay Rates of the Umbral Area of Sunspot Groups Using a High-resolution Database. *Astrophys. J.*, **892**, 107.
Muraközy, J.: 2021, On the Decay of Sunspot Groups and Their Internal Parts in Detail. *Astrophys. J.*, **908**, 133.
Muraközy, J.: 2022, Variations of the Internal Asymmetries of Sunspot Groups during Their Decay. *Astrophys. J.*, **925**, 87.
Nagovitsyn, Y.A.: 2007, Solar Cycles during the Maunder Minimum *Astronomy Letters*, **33:5**, 340.
Nagovitsyn, Y.A., Osipova, A.A., Nagovitsyna, E.Y.: 2021, "Generative" Indices of Sunspot Solar Activity: 145-Year Composite Series. *Solar Phys.*, **296**, 32.
Nagovitsyn, Y.A., Osipova, A.A.: 2021, Average annual total sunspot area in the last 410 years: The most probable values and limits of their uncertainties. *Mon. Not. Roy. Astron. Soc.*, **505**, 1206.
Nandy, D., Martens, P.C.H., Orbidko, V., Dash, S., Georgieva, K.: 2021, Solar evolution and extrema: Current state of understanding of long-term solar variability and its planetary impacts. *Prog. Earth and Planetary Sci.*, **8**, # 40.
Obridko, V.N., Shelting, B.D.: 2007, Occurrence of the 1.3-year periodicity in the large-scale solar magnetic field for 8 solar cycles. *Adv. Space Res.*, **40**, 1006. https://doi.org/10.1016/j.asr.2007.04.105
Owens, M.J., Lockwood, M., Hawkins, E., Usoskin, I., Jones, G.S., Barnard, L., Schurer, A., Fasullo, J.: 2017, The Maunder Minimum and the Little Ice Age: An update from recent reconstructions and climate simulations. *Rev. Geophys.*, **48**, RG4001.
Perez-Peraza, J., Velasco, V., Libin, I. Ya., Yudakhin, K.: 2012, Thirty-year periodicity of cosmic rays. *Advances in Astronomy* **# 691408**, 11.
Pevtsov, A.A., Bertello, L., Nagovitsyn, Y.A., Tlatov, A.G., Pipin, V.V.: 2021, Long-term studies of photospheric magnetic fields on the Sun. *J. Space Weather Space Clim.*, **11**, 4. https://doi.org/10.1051/swsc/2020069
Polygiannakis, J., Preka-Papadema, P., Moussas, X.: 2003, On signal-noise decomposition of time-series using the continuous wavelet transform: application to sunspot index. *Mon. Not. Roy. Astron. Soc.*, **343**, 725.
Rempel, M., Schlichenmaier, R.: 2011, Sunspot Modeling: From Simplified Models to Radiative MHD Simulations. *Living Rev. Sol. Phys.* **8**, 3.
Ribes, J.C., Nesme-Ribes, E..: 1993, The solar sunspot cycle in the Maunder minimum AD 1645 to AD 1715. *Astron. Astrophys.*, **276**, 549.
Rieger, E., Share, G.H., Forrest, D.J., Kanbach, G., Reppin, C., Chupp, E.L.: 1984, A 154-day periodicity in the occurrence of hard solar flares? *Nature*, **312**, 623.
Schwabe, H.: 1844, Sonnen-Beobachtungen im Jahre 1843. *Astron. Nachr.*, **21**, 233.
Silverman, S.M.: 1992, Secular variation of the aurora for the past 500 years. *Rev. Geophys.*, **30**, 333. https://doi.org/10.1029/92RG01571
Simpson, J.: 2020, Naked-eye sunspot observations: A critical review of pre-telescopic western reports. *J. Br. Astron. Assoc.*, **130**, 15.
Solanki, S.K.: 2003, Sunspots: An overview. *Astron. Astrophys. Rev.*, **11**, 153.
Solanki, S.K., Krivova, N.A., Haigh, J.D.: 2013, Solar Irradiance Variability and Climate. *Annual Rev. Astron. Astrophys.*, **51**, 311.
Soon, W., Frick, P., Baliunas, S.L.: 1999, Lifetime of surface features and stellar rotation: A wavelet time-frequency approach, *Astrophys. J.*, **510**, L135.
Soon, W., Yaskell, S.H.: 2003, The Maunder Minimum and the Variable Sun-Earth Connection. *World Scientific Publishing Co. Pte. Ltd.*
Soon, W., Velasco Herrera, V., Selvaraj, K., Traversi, R., Usoskin, I., Chen, C.-T.A., Lou, J.-Y., Kao, S.-J., Carter, R.M., Pipin, V., Severi, M., Becagli, S.: 2014, A review of Holocene solar-linked climatic variation on centennial to millennial timescales: Physical processes, interpretative frameworks and a new multiple cross-wavelet transform algorithm. *Earth-Science Reviews*, **134**, 1.
Soon, W., Velasco Herrera, V. M., Cionco, R. G., Qiu, S., Baliunas, S., Egeland, R.: 2019, Covariations of chromospheric and photometric variability of the young Sun analogue HD 30495: evidence for and interpretation of mid-term periodicities. *Mon. Not. Roy. Astron. Soc.*, **483**, 2748.
Soon, W., Connolly, R., Connolly, M., Akasofu, S.-I., Baliunas, S., Berglund, J., Bianchini, A., Briggs, W.M., Butler, C.J., Cionco, R.G., Crok, M., Elias, A.G., Fedorov, V.M., Gervais, F., Harde, H., Henry, G.W., Hoyt, D.V., Humlum, O., Legates, D.R., Lupo, A.R., Maruyama, S., Moore, P., Ogurtsov, M., ÓhAiseadha, C., Oliveira, M.J., Park, S.-S., Qiu, S., Quinn, G., Scafetta, N., Solheim, J.-E., Steele, J., Szarka, L., Tanaka, H.L., Taylor, M.K., Vahrenholt, F., Velasco Herrera V.M., Zhang, W.: 2023, The Detection and Attribution of Northern Hemisphere Land Surface Warming (1850–2018) in Terms of Human and Natural Factors: Challenges of Inadequate Data. *Climate*, **11**, 179. https://doi.org/10.3390/cli11090179
Spörer, G.: 1887, Ueber die Periodicität der Sonnenflecken seit dem Jahre 1618, vornehmlich in Bezug auf die heliographische Breite derselben, und Hinweis auf eine erhebliche Störung dieser Periodicität während eines langen Zeitraumes. *Vierteljahrsschr. Astron. Ges.*, **22**, 323.
Stefani, F., Giesecke, A., Weier, T.: 2019, A model of a tidally synchronized solar dynamo. *Solar Phys.*, **294**, # 60.
Švanda, M., Brun, A.S., Roudier, T., Jouve, L.: 2016, Polar cap magnetic field reversals during solar grand minima: could pores play a role? *Astron. Astrophys.*, **586**, A123. 10.1051/0004-6361/201527314
Thomas, J.H., Weiss, N.O.: 2004, Fine Structure in Sunspots. *Annual Rev. Astron. Astrophys.*, **42**, 517.
Tlatov, A.G., Vasil'eva, V.V., Makarova, V.V., Otkidychev, P.A.: 2014, Applying an automatic image processing method to synoptic observations. *Solar Phys.*, **289**, 1403.
Tlatov, A.G., Petsov, A.A.: 2017, On the timing of the next great solar activity minimum. *Adv. Space Res.*, **60 (5)**, 1108. https://doi.org/10.1016/j.asr.2017.05.009
Tlatov, A.G.: 2022a, Dark Dots on the Photosphere and Their Counting in the Sunspot Index. *Solar Phys.*, **297**, 67. https://doi.org/10.1007/s11207-022-02002-8
Tlatov, A.G.: 2022b, The Shape of Sunspots and Solar Activity Cycles. *Solar Phys.*, **297**, 110. https://doi.org/10.1007/s11207-022-02045-x
Torrence, C., Compo, G.: 1998, A practical guide to wavelet analysis. *Bulletin of American Meteorological Society*, **79**, 61.
Trillas, E., Eciolaza, L.: 2015, Fuzzy Logic. *Springer, New York*, **320**, 211.
Usoskin, I., Solanki, S., Kovaltsov, G., Beer, J., Kromer, B.: 2006, Solar proton events in cosmogenc isotope data. *Geophys. Res. Lett.*, **33**, L08107. https://doi.org/10.1029/2006GL026059
Usoskin, I.G., Arlt, R., Asvestari, E., Hawkins, E., Kapyla, M., Kovaltsov, G.A., Krivova, N., Lockwood, M., Mursula, K., O'Reily, J.O., Owens, M., Scott, C.J., Sokoloff, D.D., Solanki, S., Soon, W., Vaquero, J.M.: 2015, The Maunder minimum (1645-1715) was indeed a grand minimum: A reassessment of multiple datasets. *Astron. Astrophys.*, **581**, A95.
Usoskin, I.G., Kovaltsov, G.A., Chatzistergos, T.: 2016, Dependence of the Sunspot-Group Size on the Level of Solar Activity and its Influence on the Calibration of Solar Observers. *Solar Phys.*, **291**, 3793.
Usoskin, G. A. Kovaltsov, Lockwood, Mursula, M.K., Owens, M., S. K. Solanki, S.K.: 2016, A New Calibrated Sunspot Group Series Since 1749: Statistics of Active Day Fractions *Solar Phys.*, **291**, 685.

Usoskin, I.G.: 2017, A History of Solar Activity over Millennia. *Living Rev. Sol. Phys.*, **14**, 3.

Usoskin, I.G., Solanki, S.K., Krivova, N., Hofer, B., Kovaltsov, G.A., Wacker, L., Brehm, N., Kromer, B.: 2021, Solar cyclic activity over the last millennium reconstructed from annual ^{14}C data. *Astron. Astrophys.*, **649**, A141.

Valdés-Galicia, J.F., Otaola, J., Pérez-Enríquez, R.: 1996, The Cosmic-Ray 1.68-Year Variation: a Clue to Understand the Nature of the Solar Cycle? *Solar Phys.*, **169**, 409.

Valdés-Galicia, J.F., Velasco Herrera, V.M.: 2008 Variations of mid-term periodicities in solar activity physical phenomena. *Adv. Space Res.*, **41**, 297.

Vaquero, J.M., Kovaltsov, G.A., Usoskin, I.G., Carrasco, V.M.S., Gallego, M.C.: 2015, Level and length of cyclic solar activity during the Maunder minimum as deduced from the active-day statistics. *Astron. Astrophys.*, **577**, A&71.

Vaquero, J.M., Svalgaard, L., Carrasco, V.M. S., Clette, F., Lefévre, L., Gallego, M.C., Arlt, R., Aparicio, A.J.P., Richard, J.G., Howe, R.: 2016, A Revised Collection of Sunspot Group Numbers. *Solar Phys.*, **291**, 3061. https://doi-org.pbidi.unam.mx:2443/10.1007/s11207-016-0982-2

Velasco Herrera, V., Mendoza, B., Velasco Herrera, G.: 2015, Reconstruction and prediction of the total solar irradiance: From the Medieval Warm Period to the 21st century. *New Astronomy*, **34**, 221.

Velasco Herrera, V.M., Soon, W., Velasco Herrera, G., Traversi, R., Horiouchi, K.: 2017, Genelizationof the cross-wavelet function. *New Astronomy*, **56**, 86.

Velasco Herrera, V.M., Perez-Peraza, J., Soon, W., Marquez-Adame, J.C.: 2018, The quasi-biennial oscillation of 1.7 years in ground level enhancement events. *New Astronomy*, **60**, 7.

Velasco Herrera, V.M., Soon, W., Legates, D.R.: 2021, Does Machine Learning reconstruct missing sunspots and forecast a new solar minimum? *Adv. Space Res.*, **68**, 1485-1501.

Velasco Herrera, V.M., Soon, W., Hoyt, D.V., Muraközy, J.: 2022a, Group Sunspot Numbers: A new reconstruction of sunspot activity variations from historical sunspot records using algorithms from Machine Learning. *Solar Phys.*, **297**, # 8.

Velasco Herrera, V.M., Soon, W., Knoska, S., Perez-Peraza, J.A., Cionco, R.G., Kudryavtsev, S.M., Qiu, S., Connolly, R., Connolly, M., Svanda, M., Acosta Jara, J., Gregori, G.P..: 2022b, The New Composite Solar Flare Index from Solar Cycle 17 to Cycle 24 (1937-2020). *Solar Phys.*, **297**, # 108.

Velasco Herrera, V.M., Martell-Dubois, R., Soon, W., Velasco, G., Cerdeira-Estrada, S., Zúñiga, E., Rosique-de la Cruz, L.: 2022c, Predicting Atlantic hurricanes using Machine Learning. *Atmosphere*, **13**, 707.

Velasco Herrera, V.M., Rossello, E.A., Orgeira, M.J., Arioni, L., Soon, W., Velasco, G., Rosique-de la Cruz, L., Zúñiga, E., Vera, C.: 2022d, Long-Term Forecasting of Strong Earthquakes in North America, South America, Japan, Southern China and Northern India With Machine Learning. *Front. Earth Sci.*, **10**, 905792.

Velasco Herrera, V.M., Soon, W., Hoyt, D., Babynets, N., Murakozy, J., Tlatov, A., Nagovitsyn, Y., Qiu, S., Svanda, M., Velasco Herrera, P.A.: 2023, Reconstruction and Emulation Solar Activity Since the Maunder Minimum Using Genetic Algorithms. *submitted*.

Wang, H., Li, H.: 2022, Rediscovery of 23 historical records of naked-eye sunspot observations in AD 1618. *Solar Phys.*, **297**, # 127.

Wu, C.J., Usoskin, I.G., Krivova, N., Kovaltsov, G.A., Baroni, M., Bard, E., Solanki, S.K.: 2018, Solar activity over nine millennia: A consistent multi-proxy reconstruction. *Astron. Astrophys.*, **615**, A93.

Yang, Z., Yang, Y., Feng, S., Liang, B., Dai, W., Xiong, J.: 2023, Sunspot extraction and hemispheric stastistics of YNAO sunspot drawings using deep learning. *Astrophys. Space Sci.*, **368**, # 2.

Yu, X., Gen, M..: 2010, Introduction to Evolutionary Algorithms. *Springer, London*, 411.

Zolotova, N.V., Ponyavin, D.I.: 2015, The Maunder Minimum is not as Grand as it Seemed to be. *Astrophys. J.*, **800**, 42. https://doi.org/10.1088/0004-637X/800/1/42

Declaration of interests

☒The authors declare that they have no known competing financial interests or personal relationships that could have appeared to influence the work reported in this paper.

☐The authors declare the following financial interests/personal relationships which may be considered as potential competing interests: